Trinity College Dublin
Coláiste na Tríonóide, Baile Átha Cliath
The University of Dublin

Understanding how community context drives virulence-associated traits in the Cystic Fibrosis pathogen *Pseudomonas aeruginosa*

Filza Masood

MSc (by Research)

Microbiology 2025

A dissertation presented for the degree of M.Sc. in the Faculty of Science, Technology, Engineering, and Mathematics, Trinity College Dublin

Supervisor: Dr Siobhán O' Brien

DECLARATION

I declare that this thesis has not been submitted as an exercise for a degree at this or any other university and it is entirely my own work.

I agree to deposit this thesis in the University's open access institutional repository or allow the Library to do so on my behalf, subject to Irish Copyright Legislation and Trinity College Library conditions of use and acknowledgement.

I consent to the examiner retaining a copy of the thesis beyond the examining period, should they so wish (EU GDPR May 2018)

I have read and I understand the plagiarism provisions in the General Regulations of the University Calendar for the current year, found at: http://www.tcd.ie/calendar.

I have completed the Online Tutorial on avoiding plagiarism 'Ready, Steady, Write', located at http://tcd-ie.libguides.com/plagiarism/ready-steady-write.

Signed: Filza Masood

Signed: Siobhán O' Brien

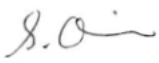

ACKNOWLEDGMENTS

I would like to express my sincere gratitude to my supervisor Dr Siobhán O' Brien for her invaluable support, guidance, and feedback throughout my research masters. I am also deeply thankful to the O'Brien research group for their time, input, and company throughout this past year; the biggest thank you to my lab mates Sadhbh, Jake, and James who became my great friends. Thank you also to the Ní Leathlobhair group for the shared EcoEvo journal club meetings and the feedback on presentations.

Thank you to my committee members Dr Carsten Kroeger and Dr Julie Renwick for their guidance and suggestions for my research. I'd also like to thank all the technical and support staff in the Moyne Institute of Preventive Medicine for their constant help and advice. Thank you especially to Connie, Miriam, Margaret, and Ciaran.

Finally, I'd like to mention some other members of the Moyne who provided constant support this past year, and who have become some of my closest friends. Thank you to Zoe, Orlaith, Kate, Rebecca, and Sophia for making me feel so welcome and for all the great Moyne memories. I couldn't have done it without you all and am truly grateful.

Table of Contents

ABSTRACT

The lungs of patients with Cystic Fibrosis (CF) are often chronically colonised by a plethora of microbial species, including the major CF pathogen *Pseudomonas aeruginosa (P. aeruginosa).* Herewith, when examining recalcitrant bacterial infections in CF, it is imperative to not only study pathogens in isolation, but rather, as part of ecological communities interacting at the species level. The successful invasion and robust virulence mechanisms of *P. aeruginosa* are influenced by members of the lung microbiome. Interspecies interactions can shape and often determine virulence evolution, mediated through synergistic and antagonistic behaviours. Moreover, species richness and composition act in concert to impact *P. aeruginosa* colonisation and may predict important clinical phenotypes – yet it is difficult in practice to tease apart the effects of diversity per se *versus* increased likelihood of encountering a key species at higher diversities. This project uses an ecological framework to disentangle the effects that community richness and community composition have on colonisation resistance in the CF airways and dissect how polymicrobial interactions shape *P. aeruginosa* virulence. By designing and implementing a modified random partition experiment, we were able to identify members of an artificially assembled microbial community that affect *P. aeruginosa* invasion and virulence-associated secretions such as pyoverdine and pyocyanin. This work provides a novel way of understanding microbial interactions in a clinical context, by applying an ecological framework to artificially assembled communities. This will pave the way for future work applying this framework to more "natural" CF microbial assemblages that closely reflect different clinical statuses of the CF lung.

1. INTRODUCTION

1.1 *Pseudomonas aeruginosa* in Cystic Fibrosis

Pseudomonas aeruginosa

Pseudomonas aeruginosa (P. aeruginosa) is Gram-negative, motile, aerobic bacterium, and one of the most prominent causes of human infectious disease. Part of the ESKAPE pathogen list [1, 2], *P. aeruginosa* has been widely known to cause persistent infections and is difficult to treat due to its intricate mechanisms of antibiotic resistance *via* acquired, adaptive, and intrinsic methods [3]. Biofilm formation, overexpression of efflux pumps, and antibiotic degrading enzymes are just some of the many ways in which this pathogen can persist successfully [3, 4].

Cystic Fibrosis

Cystic Fibrosis (CF) is an autosomal recessive disorder and the most common inherited disorder in Ireland, primarily affecting the lungs and digestive system. Mutations in the Cystic Fibrosis Transmembrane conductance Regulator (CFTR) gene lead to aberrant sodium and calcium ion transport, resulting in thick mucus accumulation and impaired mucociliary clearance, creating an environment conducive to infections [5]. The mucus build-ups serve as a reservoir of bacterial infections, a replicative niche in which pathogens can thrive [6]. Polymicrobial interactions, where multiple microbial species coexist, are of particular significance in the context of CF. These interactions can have complex implications for disease progression, treatment, and patient outcomes [6].

Environmentally-acquired *P. aeruginosa* infections are of great clinical importance in immunocompromised CF patients [7]. Its initial colonisation leads to a chronic persistent infection, which is a significant milestone in disease progression [8]. This pernicious infection in the lungs is often due to a multispecies biofilm mode of growth which dampens antibiotic efficacy [9]. *P. aeruginosa* displays a remarkable ability to adapt to the CF lung environment, with isolates from long-term chronic infections being phenotypically distinct from acute, more virulent isolates [10]. During chronic CF lung infections, *P. aeruginosa* undergoes a somewhat predictable trajectory of evolutionary adaptation, including loss of virulence factors, transition to a biofilm lifestyle, hypermutability, and increased antibiotic resistance [10, 11]. Together, these adaptations, combined with extensive within-patient diversity [12] and intricate polymicrobial interactions [5, 13], prove a hindrance to pathogen targeting and eradication.

1.2 Cystic Fibrosis as a polymicrobial disease

Many diseases encompass a polymicrobial aetiology and the airways of CF patients are a pertinent example of this, harbouring diverse microbial ecosystems that can affect therapeutic interventions and outcomes [5, 14]. Therefore, it is crucial to probe infection from a polymicrobial and ecological lens, as would be representative of what is occurring *in vivo* [15]. Bacterial species found in the lung include *Staphylococcus* spp., *Streptococcus* spp., *Burkholderia cepacia* complex (BCC), and also include oral commensals such as *Rothia mucilaginosa (R. mucilaginosa)* and *Rothia dentocariosa (R. dentocariosa)*, as well as fungi such as *Candida* and *Aspergillus* species [16]. Other notable microbes include *Haemophilus influenzae*, *Stenotrophomonas maltophilia*, *Achromobacter xyloxidans*, and *Mycobacterium abscessus* [5].

A growing body of evidence is showing that interactions between *P. aeruginosa* and other members of the CF lung community are relevant for clinically important traits such as virulence and antimicrobial resistance (AMR). While species such as *Staphylococcus aureus* and BCC have been shown to actively compete with, and in some cases inhibit *P. aeruginosa* growth via iron competition [17, 18], interactions with *R. mucilaginosa* have been recently shown to boost *P. aeruginosa* growth [19]. Despite tantalising evidence that community context shapes *P. aeruginosa* virulence and/or AMR, studies typically either; a) focus on just one or two species, or b) focus on change in gene regulation in *P. aeruginosa*, rather than evolved responses to CF microbiota [20]. This is an attractive approach, because it permits detailed and important molecular studies of often well-characterised isolates – yet applicability to the complex and dynamic nature of natural microbial communities may be limited.

Community diversity/composition has also been shown to play an important role in driving CF lung microbiota changes during pulmonary exacerbations, suggesting possible predictions of *P. aeruginosa* burden and clinical outcomes [21]. There is evidence that CF community context also holds implications for the ability of *P. aeruginosa* to invade and colonise the airways [22]. Microbial ecology studies predict that more diverse communities tend to have colonisation resistance, and *via* mechanisms such as nutrient blocking, can impede the ability of pathogens to establish infections [22]. In CF, more diverse communities tend to be less likely to harbour *P. aeruginosa,* supporting the idea that community diversity can constrain this pathogen's invasion. However, it is unclear whether diversity *per se* is the key factor promoting colonisation resistance, or if richer communities are simply more likely to contain a particular species/taxa that inhibits *P. aeruginosa,* thereby, community composition being a more pertinent factor. Teasing apart the effects of diversity *versus* composition is not a straightforward task, as it requires large manipulations of synthetic communities in which every single reciprocal interaction is tested and replicated multiple times. In this study, we use an ecological framework (random partition design) to pull apart the relative contribution of community composition versus diversity on *P. aeruginosa* invasion and virulence.

1.3 The Lung microbiome: Healthy *versus* CF

Up until a few decades ago, the lungs were thought to be sterile and free from microorganisms [23]. However, we now know that the lungs harbour diverse microbial communities [24]. These microbes residing in the upper and lower respiratory tract play a significant role in maintaining respiratory health, contributing to metabolic homeostasis and colonisation resistance against pathogens [23, 24]. The healthy lung microbiome consists of bacteria from the genera *Streptococcus* spp., *Staphylococcus* spp., *Veillonella* spp., *Prevotella* spp., fungal species such as *Aspergillus* spp, and *Candida* spp, and also respiratory viruses such as rhinoviruses [24].

The dynamic lung environment undergoes many changes during CF infection, creating a low-oxygen, nutrient-rich, and highly inflammatory niche for microbes to persist [25]. The thick mucus build-up in the airways often creates a physical barrier impairing oxygen diffusion from the airway lumen to the underlying cells and microbes. Moreover, chronic bacterial infections in the CF lungs trigger a pro-inflammatory response. The recruitment of immune cells such as neutrophils to the sites of infection consumes oxygen, further decreasing oxygen availability in the mucus and surrounding tissue [26]. Some anaerobic bacteria can also create low-oxygen microenvironments, especially when in multispecies biofilms with *P. aeruginosa* [27].

The lung microbiome in patients with CF (pwCF) is typically less diverse than healthy individuals due to the selective pressure exerted by forces such as repeated antibiotic use, as well as the dominance of highly adapted pathogens such as *P. aeruginosa* and *S. aureus* [16]. The polymicrobial nature of CF infections results in biofilm formation – complex communities of bacteria embedded in a self-produced matrix of extracellular polysaccharide. *P. aeruginosa* is known to adapt this sessile biofilm lifestyle in the CF lung which enhances its survival and confers protection against antibiotics [11, 20].

The CF respiratory tract comprises of the normal lung microbiota with shifts in relative abundance and richness as infections persist. The presence of oral and nasal commensals in sputum isolated from pwCF resulting from aspiration into the lower respiratory tracts is also seen [28] . While the link between the oral and lung microbiomes in CF has not been studied in depth, it is known that oral microbiota can be a source of opportunistic pathogens that migrate to the respiratory tract and cause infection [29, 30].

P. aeruginosa undergoes a switch from an aerobic to an anaerobic environment in the CF lung and this switch can introduce metabolic changes but also alterations in virulence factor production as these are closely coupled [31] . With the added factor of other microbial species, these changes can be difficult to predict when it comes to changes in antibiotic susceptibility, biofilm formation, and phenazine and siderophore production [32]. It is therefore important to consider whether the pathogen is in an aerobic, anaerobic, or even microaerophilic environment [27]. *P. aeruginosa* has great metabolic flexibility and

during anoxic or hypoxic conditions, can rely on nitrate sources [27]. However, this metabolic flexibility may be enhanced or even obstructed by the presence of other microbial community members in the CF airways.

1.4 Polymicrobial interactions

Polymicrobial interactions are key features of microbial communities. Species may facilitate another's growth, for example *via* the secretion of "leaky metabolites"[33], public goods, and antibiotic-degrading enzymes. Such facilitation has been proposed to play a role in CF microbial communities. For example, anaerobic bacteria such as *Streptococcus* spp. can create an anoxic environment which may be favourable to *P. aeruginosa* [34]. Iron-chelating siderophores may also be shared between some species, allowing a second species to grow when iron is unavailable [35-37]. However, while there is evidence for facilitation operating between species, this is largely based on pulling species out of their natural environment and testing in artificial conditions. It is still under debate as to whether facilitation plays a role in more complex microbiota, where populations are spatially structured and there is substantial within-species diversity.

Competition is prevalent within microbial communities, and can typically result in bacteriostatic/bactericidal behaviours [17]. Microbes competing for the same ecological niche or nutrients may employ tactics such as producing toxins or siderophores, to outcompete or kill neighbouring competitors [28, 33]. The somewhat harsh CF environment requires bacteria to rapidly adapt to both the host as well as the bacterial community to survive and persist [38, 39]. Many CF pathogens communicate through quorum sensing, modulating their behaviours based on population density and environmental stimuli. This is particularly important in biofilm formation, a hallmark of recalcitrant CF infections and increased antibiotic resistance within the CF lung [38, 40, 41].

In this project, a combination of six microbial species (five bacterial, one fungal) that have been previously identified in the CF lung were used. Due to practical constraints, these species are all aerobes, but the experimental framework employed here could equally be applied to anaerobes or a mix of aerobes and anaerobes. Below is a short description of the role each species plays in CF lung, as well as how each species might be expected to interact with *P. aeruginosa.*

1.4.1 S. *aureus*

The interactions between the Gram-positive pathogen *S. aureus* and *P. aeruginosa* in CF is perhaps one of the most widely studied and characterised [42]. It was widely accepted that *S. aureus* was the dominant pathogen in the early years of pwCF and was often outcompeted and displaced by *P. aeruginosa* in teenage years [6, 43]. For a long time, this competitive interaction was the only one considered. More recently, several studies [44-46] have described that the two prevalent species can co-exist. This change in dynamics is linked to evolution of bacterial strains in the CF lungs and changes the impact of infection and treatment, yet again proving the need to study CF infection and dynamic polymicrobial interactions, constantly undergoing evolutionary changes. An interaction that has been extensively studied, is how *S. aureus* influences *P. aeruginosa* pyocyanin production [47]. *S. aureus* and *P. aeruginosa* can coexist within polymicrobial biofilms in the CF lung. The presence of *S. aureus* and its secreted metabolites may alter the local microenvironment, altering nutrient availability, resulting in metabolic changes [31] that may induce *P. aeruginosa* pyocyanin expression as a response to environmental stressors [45].

1.4.2 *S. epidermidis* and *S. hominis*

The upper respiratory tract harbours a bacterial community residing in the nasopharyngeal cavity. This microbiota protects against respiratory pathogens, providing colonisation resistance [30]. While having previously been described as commensals of the normal skin and mucosal microbiota in humans, *S. epidermidis* and *S. hominis* have been shown to behave like an opportunistic pathogen, with *S. epidermidis* being involved in many healthcare associated infections, particularly associated with biofilm formation on medical devices [48]. These Gram-positive, coagulase negative coccus species may possibly interact with *P. aeruginosa,* competing for replicative niches, or affecting *P. aeruginosa* growth via secretion of bacteriocins such as hominicin in the case off *S. hominis* [49-51]. We can speculate that many interactions may take place between *P. aeruginosa* and these staphylococcal species, especially when all three members are in coculture. These may include competition for nutrients in the replicative niche, biofilm formation, or the use of public goods such as siderophores and overall impact community dynamics and *P. aeruginosa* virulence.

1.4.3 *R. mucilaginosa* and *R. dentocariosa*

When it comes to lung conditions like CF, the oral microbiota might be a neglected source of infection. Although little is known about the oral-lung axis, we do know that commensals from the oral microbiota can be inhaled into the lungs' and upper respiratory microbiota's airways, especially in CF, with sputum isolated from pwCF originating from aspiration into the lower respiratory tracts containing oral and nasal commensals [29]. Opportunistic bacteria that move to the respiratory system and cause infection can also originate from the mouth microbiota (35, 50). Gram-positive *Rothia* spp. are common dwellers

of the oral microbiome, but we know little to nothing about their potential role in CF. While not pathogenic themselves, we can hypothesise once aspirated into the upper airways, they may interact with *P. aeruginosa via* secreted metabolites as was shown in the case of *R. mucilaginosa* [19]. *R. mucilaginosa* was also recently shown to produce the metal-chelator enterobactin [52], which can strengthen our hypothesis that it plays a role in *P. aeruginosa* infections in CF due to the pathogen's well studied need for iron in CF [53, 54].

1.4.4 *C. albicans*

The interactions between *P. aeruginosa* and fungal species, particularly *C. albicans,* in the context of CF lung infections has been a topic of interest in recent years. *C. albicans* has been shown to modulate *P. aeruginosa* virulence in many ways, both by direct nutrient blocking via iron competition, and indirectly disrupting regulatory networks of metabolite production. One way it does this is by producing the ethanol farnesol [55]. This molecule has been shown to interfere with the quorum sensing (QS) systems of *P. aeruginosa* [56]. QS is essential for bacteria to communicate and respond based on environmental stimulus, serving as the basis of coordinating virulence factor expression and initiating biofilm formation in many bacterial species. Unlike *S. aureus* increasing pyocyanin production, farnesol may inhibit expression of pyocyanin production via QS disruptions, thereby attenuating *P. aeruginosa* pathogenicity [57]. Farnesol has also been shown to impact metabolism of *P. aeruginosa* affecting its growth and survival in the CF lung [58].

1.5 Applying ecological theory to understand colonisation resistance in the CF lung

Natural microbial communities contain hundreds to thousands of species interacting on various levels. For this reason, computational studies to model polymicrobial disease *in silico,* have become increasingly popular in the field of microbial ecology to model and map out these interactions to assist in predictive analysis, which can only be achieved by understanding the complex interactions that are at play [59].

Many studies using artificially assembled two-species microbial communities have shown interspecies interactions can drive important clinical phenotypes in *P. aeruginosa*, such as virulence and antibiotic resistance [13, 60] . However, natural bacterial communities, particularly within the host, contain many species engaging in complex webs of interactions. Modelling these interactions is no easy feat, and things become even more difficult when trying to recreate these complex and dynamic communities in the laboratory environment. However, the field of ecology has been focused on understanding natural communities for decades, including the effect of species richness and diversity on the success of an

invasive species, for example. Hence, understanding CF microbial communities may be facilitated by bridging the gap between clinical microbiology and ecology. In 2009, Thomas Bell and colleagues [61] developed a model to unpick the relative importance of community richness and composition on some attribute of community function (e.g. colonisation resistance, respiration), without the need to perform reciprocal interaction experiments with all members of a synthetic community. It is important to distinguish that species richness/diversity refers to how many species are present in a community and species composition refers to exactly what species are present and their identities. In the Bell [61] model, a random partition design coupled with linear models are used to test the relative contribution of each species to community function. An illustration of the experimental design is given in **Fig. 1.**

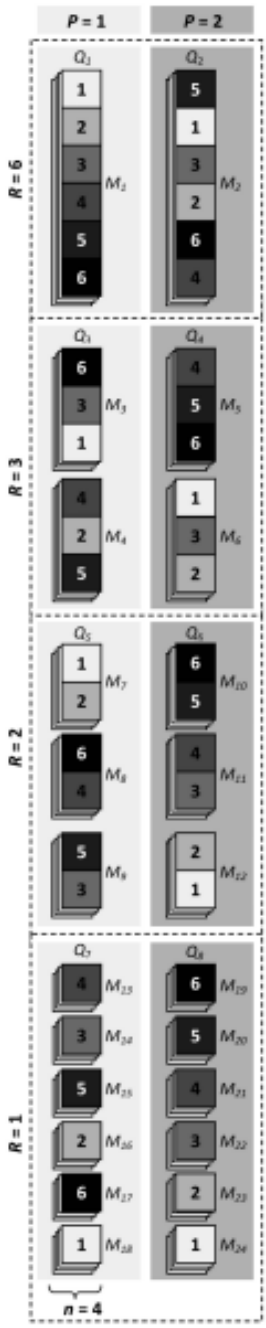

Fig. 1. Experimental design of the random partition model. Schematic taken from key paper by Thomas Bell (2009) [61]. Each square is a species, with the numbers designating whether it is species 1, 2, 3, 4, 5, or 6.

For an experiment with a species pool of S species, let $\delta = \{R_1, R_2, \ldots, R_d\}$ be the set of all whole number factors of S, where $R_1 \ldots R_d$ is the number of species at each of the d richness levels. The vector δ therefore defines the species richness levels used in the experiment. For example, in this experimental setup, if $S = 6$, then $\delta = \{1, 2, 3, 6\}$ and $d = 4$.

In our study, species are designated with a letter A, B, C, D, E, or F

A	*Candida albicans*
B	*Staphylococcus aureus*
C	*Staphylococcus hominis*
D	*Staphylococcus epidermidis*
E	*Rothia dentocariosa*
F	*Rothia mucilaginosa*

This idea has been primarily applied to soil microbe studies [62-66] with broader investigations into phytoplankton importance in ecosystem functioning [67], highlighting how generally applicable this model can be. Despite this, this model has not yet been applied to microbes of clinical relevance in human disease. Here, we modified and applied this model to understand how CF community diversity and composition affect *P. aeruginosa* colonisation resistance, using a synthetic community containing six species. Communities will be established and left to stabilise overnight, before adding in *P. aeruginosa* and seeing how each community fares in its ability to prevent growth by this CF pathogen. Using this design, we aim to identify key species/communities affecting *P. aeruginosa* invasion ability, biofilm formation, virulence factor production, and AMR. Due to time constraints, we have focused solely on the effect background species might have on *P. aeruginosa*, although acknowledge that *P. aeruginosa* may in turn impact clinically relevant traits in background species Finally, while the experiments are typically performed in simple lab media, we also test whether findings are similar in artificial sputum. While the work presented here provides proof-of-concept that ecological framework could be useful in CF microbiology, it will also guide future longer-term work that applies this framework in natural, more complex CF communities, potentially in lab environments that mimic CF conditions such as ASM or a mouse model.

1.6 Scope of this study

This project aimed to combine ecological theory and coculturing of synthetic bacterial communities to understand how community context may drive evolution of clinically relevant phenotypes in the CF pathogen *P. aeruginosa*. Phenazine and siderophore production, as well as biofilm formation are three well-established traits that are associated with worsening clinical outcomes in CF [13, 44]. We have incorporated these into this study to see how community context can alter these virulence factors and secretions, to ultimately see how interactions between *P. aeruginosa* and other community members of the lung microbiome can shape and drive virulence and help predict clinically relevant phenotypes and outcomes. The effects of community context on *P. aeruginosa* final densities short-term, long-term are investigated and the evolution of clinically relevant phenotypes examined, by quantifying changes in secreted virulence factors, biofilm formation, and antimicrobial resistance.

2. METHODS

2.1 Strains

2.1.1 Focal Species: *Pseudomonas aeruginosa*

For *Pseudomonas aeruginosa*, the PAO1 strain was used (ATCC 15692, isolated from a burn wound). The Liverpool Epidemic Strain (LES) B58 was used as a Cystic Fibrosis (CF) strain to compare against the CF-naïve PAO1 isolate. Two deletion mutants derived from PAO1 were used; the isogenic mutant strain, PAO1Δ*PvdD*Δ*PchEF* which has a knockout of both primary and secondary siderophores, pyoverdine and pyochelin, and the phenazine mutant, PAO1Δ*phzABCDEFG* which lacks the phenazine biosynthetic operon phzABCDEFG (provided by Prof Steve Diggle, Georgia Tech). *P. aeruginosa* CF isolates CF03-i3, CF03-i4, CF03-i6, CF0i9, CF0i19, CF0i21, CF0i23, CF0i28, CF0i29, CF0i30, CF0i35, and CF0i37, (where CF03 is patient ID from the paper cited below, and "i" is the isolate number), were also used in this study [68]. These isolates all differ in their pyocyanin-producing abilities [12] .CF isolates were provided by Prof Joanne Fothergill (University of Liverpool).

2.1.2 Background community

Synthetic communities were constructed from six species: *Staphylococcus aureus (S. aureus), Staphylococcus hominis (S. hominis), Staphylococcus epidermidis (S. epidermidis), Candida albicans (C. albicans), Rothia mucilaginosa (R. mucilaginosa), and Rothia dentocariosa (R. dentocariosa),* all provided by Prof Joanne Fothergill (University of Liverpool). All strains were grown from glycerol stocks overnight in 6mL Brain Heart Infusion (BHI) broth. Cultures were grown shaken at 180rpm and 37°C for 20 hours.

2.2 Testing the effect of individual community species supernatant on *P. aeruginosa* growth

2.2.1 Preparation of supernatant

The six background community species, PAO1, and LESB58 were all individually grown from freezer stocks in 6ml BHI for 20 hours at 37°C, shaken at 180 rpm. The Optical density (OD; A_{600}) was measured using a Biotek Epoch 2 plate reader. Cultures were standardised to an OD of 0.5 (~$1x10^8$ cells) [69] in BHI broth, and 1ml of standardised culture was then transferred into a 1.5ml sterile Eppendorf tube. Supernatants were freshly prepared before use. Supernatants were collected by centrifugation at 8,000 x g for 4 minutes (Thermo Biosciences Micro CL 21 centrifuge), followed by filter sterilisation using a 2ml syringe (BD Emerald), and a 0.22μm PES syringe filter (Starlab).

2.2.2 Growth assays

PAO1 and LESB58 were each grown in 6ml BHI for 20 hours at 37°C, shaken at 180 rpm. OD_{600} was standardised to 0.5 following a further 1:100 dilution in BHI broth (~$1x10^5$ cells). In a 96-well microtitre plate, 20µL of the standardised PAO1 was added to 21 wells containing 120µL BHI broth. 60µL of each background species supernatant was then added to these wells in triplicate (6 species x 3 wells each). Three wells contained 180µL fresh BHI and PAO1 as a supernatant-free control. To minimise evaporation, 180µL of BHI was added to outer wells of the plate and these also acted as sterile controls. The above procedure was repeated in another plate for standardised LESB58 culture using the same supernatants and experimental setup. Growth curves were obtained by using a Biotek Epoch 2 plate reader where OD_{600} measurements were recorded every 15 minutes for 24 hours at 37°C. Plates were shaken before each recording.

2.3 Short-term Random Partition Model: How do background microbial community richness and composition impact *P. aeruginosa* final densities after 20h?

We first investigated how community context (both species composition and richness), impacts final cell densities of *P. aeruginosa* (PAO1) after 24 hours of growth with synthetic CF communities. Strains were grouped into microbial communities of six species (S=6) with species richness levels (R) of R=1, R=2, R=3, and R=6 using a random partition design described by Bell *et al.* [61]. At richness levels 2 and 3, each species was selected exactly once per partition. For example, for two-species communities (R=2), partition 1 contains three sets of species, randomly assigned into pairs (e.g. A+E, B+C, D+F). For three-species communities (R=3), partition 1 contains two sets of three species selected at random (e.g. B+C+D, A+F+E). The partition process (randomly assigning species into richness sets) was performed twice. Each partition was unique; combinations were never repeated (Table 1). For richness level = 1, all six species were tested individually, and for richness level = 6, all six species were grown together. Each community was replicated twice, except the single species, which were replicated four times (technical replicates) and together, this gave 48 communities in a single 96-well plate (24 per partition). In addition to the 48 communities, PAO1 was grown alone in triplicate without any community species as a control (48+3) (**Fig. 2**). The same experiment was repeated weekly for three weeks, providing three biological replicates per community composition.

To initiate the communities, overnight cultures of representative strains were standardised to OD_{600} = 0.1, before further diluting 1:100 in BHI. Experiments were performed in 96 well plates. For communities where R =1, 180µL of the relevant diluted culture was added to each well. For

communities where R =2, R=3 and R =6, 90µL, 60µL or 30µL of each species was added, respectively. Hence, the total bacterial volume added to each well was constant. BHI was added to outer wells to reduce evaporation (**Fig. 2**). The plate was incubated statically at 37°C for 20 hours. Following incubation, the presence of individual community members was confirmed by selective plating on Mannitol Salt Agar (MSA), *Rothia mucilaginosa* Selective Media (RMSM), and Sabouraud Dextrose Agar (SDA). Following this, 20µL of PAO1 culture, was added to every community at an initial density of $1x10^6$ CFU/ml. Communities were then returned to the incubator for 20 hours at 37°C, after which, each community was serially diluted and plated onto *Pseudomonas* base agar supplemented with C-N to allow final PAO1 densities to be calculated. Again, the presence of background community members after PAO1 treatment was confirmed by selective plating.

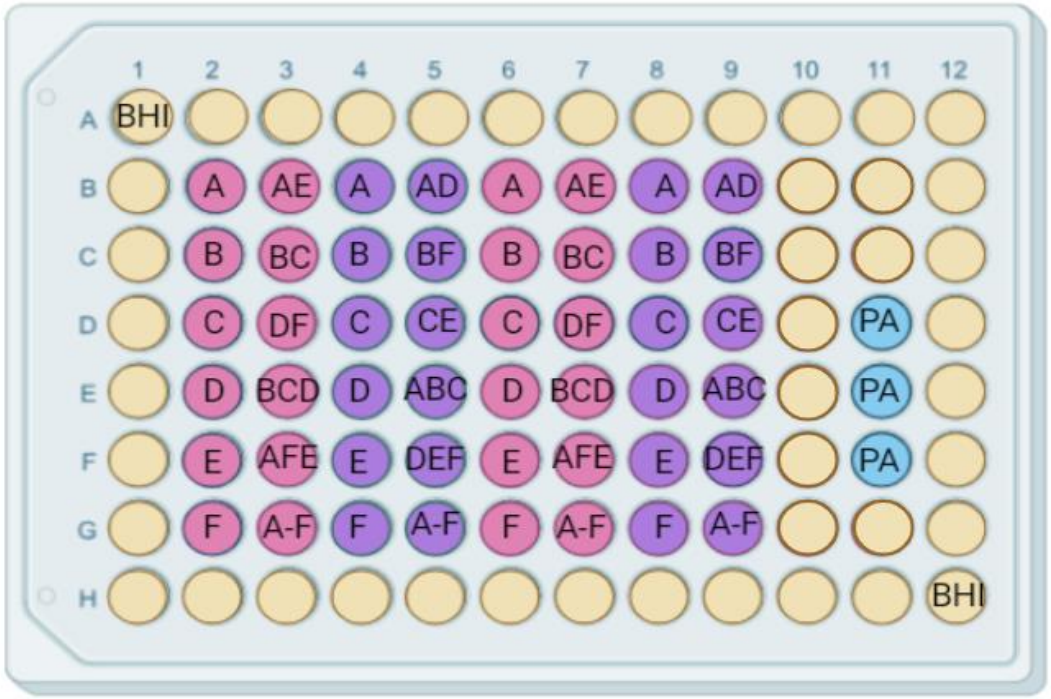

Fig. 2. Schematic of 96-well plate layout for short term random partition. Outer wells contained BHI broth to minimise evaporation (yellow). Partition 1 (Pink) and partition 2 (purple) were replicated twice. This gave two technical replicates for each two-, three-, and six-species community, and four technical replicates for each single species community. PAO1 was grown alone without any community in triplicate (blue). This experiment was repeated three times independently with the same set up as shown to give three biological replicates of each community and PAO1.

Table 1: Partition communities and their respective community IDs where R represents richness level and C represents combination, e.g., R2C1 = Richness 2, two species other than *P. aeruginosa*, Combination 1. The communities with richness levels 1 and 6 are present in partitions 1 and 2 as their community combinations cannot change. Partition 1 and 2 each contain unique sets of richness 2 (3 communities with 2 species each), and richness 3 (2 communities with 3 species each) combinations without replacement. Every single possible combination was tested with various partition set ups, but for the purpose of the model and this thesis, only two partitions are shown as this should be enough to predict trends using the Bell random partition model. *Species key: CA= Candida albicans, SA= Staphylococcus aureus, SH= Staphylococcus hominis, SE= Staphylococcus epidermidis, RD= Rothia dentocariosa, RM= Rothia mucilaginosa*

Community ID	Partition number	Combination	Species
R1C1	1 + 2	A	CA
R1C2	1 + 2	B	SA
R1C3	1 + 2	C	SH
R1C4	1 + 2	D	SE
R1C5	1 + 2	E	RD
R1C6	1 + 2	F	RM
R2C1	1	AE	CA+RD
R2C2	1	BC	SA+SH
R2C3	1	DF	SE+RM
R3C1	1	BCD	SA+SH+SE
R3C2	1	AFE	CA+RM+RD
R2C4	2	AD	CA+SE
R2C5	2	BF	SA+RM
R2C6	2	CE	SH+RD
R3C3	2	ABC	CA+SA+SH
R3C4	2	DEF	SE+RD+RM
R6C1	1 + 2	A,B,C,D,E,F	CA,SA,SH,SE,RD,RM

2.4 Extended (10-day) Random Partition Model: How do background microbial community richness and composition impact *P. aeruginosa* emergence of clinically relevant traits?

Note: We use the term "evolution" here as 10-day extended partition was aimed to be a short-term evolution experiment due to the fact that ten days is sufficient for *P. aeruginosa* to undergo pathoadaptive mutations. This study only assessed phenotypic traits and so we cannot say if these are evolved genetic adaptations. We use "evolution" here to imply changes in trajectories and emergence of different clinically relevant traits.

2.4.1Extended (10-day) Random Partition Model: Experimental setup

While the previous experiment tested how *P. aeruginosa* growth is affected by community context, the timeframe of 20 hours was not sufficient to allow *P. aeruginosa* to undergo evolutionary changes in response to community context. To test how community context shapes *P. aeruginosa* evolution of clinically relevant phenotypes, we used the same partition design but extended the experimental timeframe to 10 days. The experiment was set up initially as described above (2.3) with communities

set up and grown overnight prior to PAO1 inoculation. However, in this experiment, communities and PAO1 were allowed to interact for 10 days during which *P. aeruginosa* may undergo coevolutionary changes in response to specific community members or richness levels. In the 10- day experiments, each community was replicated twice, including PAO1 grow on its own without any community (**Fig. 3**). This resulted in 36 communities (18 x 2 communities independently evolving biological replicates). There were no technical replicates in this setup. (**Fig. 3**).

Communities were transferred to fresh BHI broth every 24 hours to stimulate growth and colonisation of nutrient rich patches. Before the transfer, the samples were thoroughly homogenised *via* aspiration using an electronic multichannel pipette as the static conditions lead to biofilm growth at the bottom of the wells. After mixing, 20µL of each community was diluted in 180µL BHI broth, before adding 20µL of this diluted community to 180µL of fresh BHI media, and incubating for 24 hours at 37°C. This yielded a 1% transfer, as per standard methods for experimental evolution [70]. This process was repeated daily until transfer 9, after which the communities were serially diluted and plated out on *Pseudomonas* base agar supplemented with C-N to allow final PAO1 densities to be calculated. The presence of all background community members was confirmed after this 10-day period by selective plating, as before. Quantitative enumeration of background species was not feasible to perform although this would be essential to determine relative abundances over this time period.

Note: Although background community species were allowed to evolve in this design (i.e. both PAO1 and community members were transferred together), investigating if or how the background community themselves evolved during the experiment was beyond the scope of this thesis. For this thesis, we focus on how evolution in the presence of varying background microbial species composition and richness shapes *P. aeruginosa* evolutionary trajectories – focusing on clinically relevant traits.

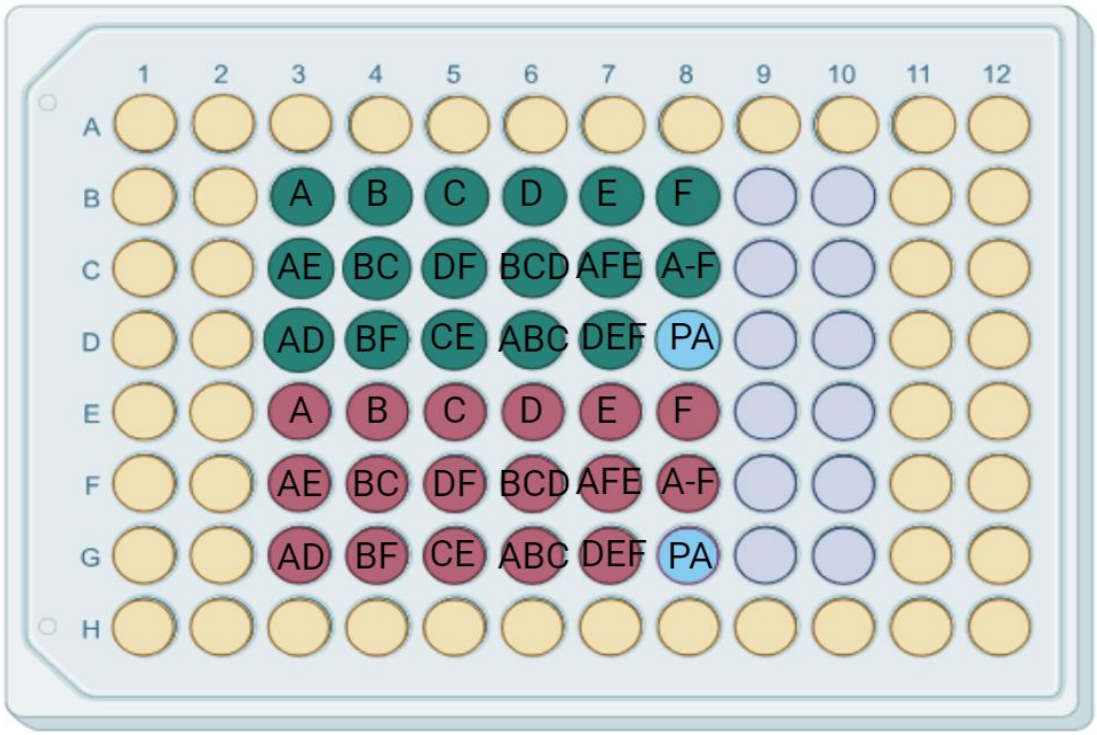

Fig. 3. Schematic of 96-well plate layout for 10-day random partition experiment. Outer wells contained BHI broth to minimise evaporation (yellow). Partitions 1 and 2, and PAO1 (blue) alone together gave 18 communities (green). These were replicated (pink) giving two independently evolving biological replicates (R1=green, R2=pink). Matching replicates in R1 and R2 were from different overnight cultures and hence were biological and not technical replicates.

2.4.2 Isolating *P. aeruginosa* from evolved communities

In order to test how community context shapes *P. aeruginosa* evolution, PAO1 was first isolated from the background communities using the following method. Each evolved community (18 x 2 reps) (Table 2) was serially diluted in Phosphate Buffer Saline (PBS). Briefly, 20µL of each community was added to 180µL of PBS. This was serially diluted 1 in 10 and 10µL of each dilution was spotted onto square plates of C-N (Cetrimide-Nalidixic acid) agar. C-N is an antibiotic supplement used to enhance the selective isolation of Pseudomonas species, particularly *Pseudomonas aeruginosa.* C-N agar was made using Pseudomonas Base agar combined with 5ml 100% glycerol with the addition of the C-N supplement vial (1vial + 1ml ddH20 + 1ml 100% ethanol). The plates were incubated at 37°C. After 18h, a sample/scrape of PAO1 was taken from each evolved population using a sterile pipette tip at the same dilution for all evolved populations (10^{-4} CFU/ml). This sample contained a snapshot of the genomic and phenotypic diversity of each evolved population, an alternative approach would have been to select multiple colonies from each population, however due to the large experimental design, this

would not have been feasible for this experiment. Evolved PAO1 population samples were inoculated into 6mL BHI and grown shaken at 180rpm and 37°C for 20 hours. Glycerol stocks (20%) were made from each evolved population by adding 600µL of bacterial culture and 400µL of 50% glycerol to cryogenic tubes. The populations were labelled as in Table 2 and stored at -80°C to be used for further phenotypic analyses.

Table 2: Evolved PAO1 populations obtained from 10-day partition experiment. The PAO1 strain refers to the unique community from which it was isolated.

Strain	Community ID/Community Isolated from
PAO1 A	R1C1 - *C. albicans*
PAO1 B	R1C2 - *S. aureus*
PAO1 C	R1C3 - *S. hominis*
PAO1 D	R1C4 - *S. epidermidis*
PAO1 E	R1C5 - *R. dentocariosa*
PAO1 F	R1C6 - *R. mucilaginosa*
PAO1 AE	R2C1 - *C. albicans, R. dentocariosa*
PAO1 BC	R2C2 - *S. aureus, S. hominis*
PAO1 DF	R2C3 - *S. epidermidis, R. mucilaginosa*
PAO1 BCD	R3C1 - *S. aureus, S. hominis, S. epidermidis*
PAO1 AFE	R3C2 - *C. albicans, R. mucilaginosa, R. dentocariosa*
PAO1 AD	R2C4 - *C. albicans, S. epidermidis*
PAO1 BF	R2C5 - *S. aureus, R. mucilaginosa*
PAO1 CE	R2C6 - *S. hominis, R. dentocariosa*
PAO1 ABC	R3C3 - *C. albicans, S. aureus, S. hominis*
PAO1 DEF	R3C4 - *S. epidermidis, R. dentocariosa, R. mucilaginosa*
PAO1 A-F	R6C1- *C. albicans, S. aureus, S. hominis, S. epidermidis, R. dentocariosa, R. mucilaginosa*
PAO1 Evo	No community, evolved in isolation

2.4.3 Quantifying clinically-relevant evolved changes in *P. aeruginosa* isolated from a 10-day partition experiment

We next examined whether evolved *P. aeruginosa* populations displayed evolutionary changes in clinically important traits (pyoverdine, pyocyanin, biofilm formation, antibiotic resistance), and if such evolutionary changes were affected by background microbial community richness and composition.

2.4.3.1 Pyocyanin measurement

To measure the phenazine pyocyanin, glycerol stocks of evolved PAO1 populations were serially diluted in PBS and plated onto C-N agar and grown for 18 hours at 37°C. A scrape of each population was taken and inoculated in 6ml Lysogeny Broth (LB), grown for 24 hours at 37°C, shaken at 180 rpm. The ancestral unevolved PAO1 was also used this assay to compare the evolved populations and evolved PAO1 against. In the results for this assay (3.3.2.1), "PAO1" refers to PAO1 passaged alone without any community, and "Ancestor" refers to the unevolved ancestral strain of PAO1. The phenazine mutant PAO1Δ*phzABCDEFG* which lacks the phenazine biosynthetic operon phzABCDEFG (provided by Prof Steve Diggle, Georgia Tech) was also used as a negative control. Overnight cultures of the ancestor and mutant strain were made in 6ml LB from glycerol stocks and also grown for 24 hours at 37°C, shaken at 180 rpm. The overnight cultures were standardised to OD 0.5 (~10^8 CFU/ml) using M9 buffer. Cultures were further diluted 1 in 100 and then 60μL of each diluted culture was inoculated into fresh 6ml LB broth grown for or 24 hours at 37°C, shaken at 180 rpm. The next day, 1ml of each culture was centrifuged at 18,000 g for 3 minutes (Thermo Biosciences Micro CL 21 centrifuge). The OD600nm was measured for each culture in triplicate and *per capita* pyocyanin was measured by measuring A_{691} for each supernatant, and then standardising by bacterial OD [12, 71]. The assay was repeated three times independently for all S1 and S2 populations, and the ancestor and mutant strains.

2.4.3.2 Pyoverdine measurement

Per capita production of the siderophore pyoverdine was measured using a pyoverdine-specific excitation-emission assay [12, 71]. Glycerol stocks of evolved PAO1 populations were serially diluted in PBS, plated onto C-N agar and grown for 18 hours at 37°C. A scrape of each population was taken and inoculated in 6ml LB grown for 24 hours at 37°C, shaken at 180 rpm. The ancestral unevolved PAO1 was also used this assay to compare the evolved populations and evolved PAO1 against. In the results for this assay (3.3.2.2), "PAO1" refers to PAO1 passaged alone without any community, and "Ancestor" refers to the unevolved ancestral strain of PAO1. The isogenic mutant strain,

PAO1Δ*PvdD*Δ*PchEF* which has a knockout of both primary and secondary siderophores, pyoverdine and pyochelin was used as a negative control. Overnight cultures of the ancestor and mutant strain were made in 6ml LB from glycerol stocks and grown for 24 hours at 37°C, shaken at 180 rpm. The OD of overnight cultures was measured at 600nm and then standardised to OD 0.5 (~10^8 CFU/ml) using M9 buffer. Cultures were then further diluted 1 in 100, and 20μL of each diluted culture was added to 180μL Casamino acid (CAA) medium in a 96-well plate in triplicate, made iron-limited by the addition of freshly prepared filter-sterilised human Apo transferrin (100 μg/ml) and sodium hydrogen carbonate (20mM $NaHCO_3$). Outer wells were filled with 200μL of CAA to reduce evaporation. Cultures were grown static for 24 hours at 37°C. The next day, cultures were mixed using a multichannel pipette and diluted 1 in 10 using PBS, before fluorescence was measured at 460nm following excitation at 400nm using a Biotek Epoch 2 plate reader. OD600nm was also measured and the ratio fluorescence/OD600 was used to give a quantitative measure of *per capita* pyoverdine production as RFU (relative fluorescence units). The assay was repeated three times independently for all S1 and S2 populations, and the ancestor and mutant strains.

2.4.3.3 Biofilm formation

Scrapes of glycerol stocks of the evolved PAO1 populations were used to inoculate 6 ml LB for 24 hours at 37°C, shaken at 180 rpm. Bacterial cultures were standardised to OD 0.1 using LB and 100μL of diluted culture was added per well in a 96-well microtitre plate in triplicate. The plate was incubated for 24-48 hours 37°C. The biofilms were stained using the crystal violet method [9, 72]. Briefly, cells are discarded by inverting and dabbing microtitre plate onto layers of paper towel and the wells are washed with PBS three times and dried to removed unattached cells. 125μL of 0.1% (w/v) crystal violet solution was added to each well and the plate incubated for 15 minutes at 37°C. The crystal violet was removed, the plate washed again with PBS. After the plate had dried, 125μL of 33% (w/v) acetic acid solution was added to each well to solubilise the crystal violet and incubated for 15 minutes at 37°C. Biofilms were quantified by reading the absorbance at 570nm using 33% acetic acid solution in a well as a blank to standardise against.

2.4.3.4 Determination of minimum inhibitory concentration

Evolved populations were tested for resistance to colistin. The minimum inhibitory concentration (MIC) of colistin was determined using the microbroth dilution method [73] in 96-well microtitre plates following EUCAST guidelines [74]. Colistin was used for this method as it cannot be used for Kirby-Bauer disc diffusion tests due to its poor diffusing ability. We still, however wanted to test this as it is

an important last-resort drug for treating *P. aeruginosa* infection. Populations were grown overnight at 37°C, shaken at 180 rpm in Mueller Hinton (MH2) broth. Optical density at 600nm (OD600) was measured and cultures were standardised to 0.5 McFarland (OD 0.8-1). Two-fold serial dilutions of a 10mg/ml colistin stock, starting at 256μg/ml were made in MH2, and both growth and sterile controls were included. The plates were incubated static for 24 hours at 37°C and then examined for growth by measuring (OD600). Growth was defined as OD600 > 0.07. The MIC values reported in Table 3 are the median of three independent biological replicates

2.4.3.5 Kirby-Bauer disc diffusion assays

Evolved populations were grown overnight at 37°C, shaken at 180 rpm in MH2 broth. OD600 was measured and cultures were standardised to 0.5 McFarland in microcentrifuge tubes. A cotton swab was then dunked into the tube and used to lawn the MH2 agar plate. The antibiotic discs were placed onto the agar within 15 minutes of spreading, in accordance with the EUCAST guidelines. The antibiotic discs were placed on the surface of the MH2 plates using an antimicrobial susceptibility disc dispenser (Oxoid). The plates were incubated for 20 hours at 37°C. The diameter of the zones of inhibition were recorded using a ruler immediately after removing the plates from the incubator. THE ATCC *E. coli* and *P. aeruginosa* strains were used as controls to ensure the discs were functioning properly. The experiment was carried out three times independently.

Note: For all phenotypic analyses, the populations termed S1 (Bio Rep 1), and S2 (Bio Rep 2) will be used, unless stated otherwise. S1 and S1 populations began as biological replicates on day 0 of the 10-day partition experiment. Each replicate (S1 and S2) contained 2 partitions; P1 and P2 (see Tables 1 and 2). As the experiment progressed with each daily passage, these replicate populations evolved differently, i.e., PAO1 isolated from R1C1 (comprising of species A, *C. albicans*) of the S1 set of populations is distinct from S2 set. This is why they will be treated as distinct evolved populations of *P. aeruginosa*, giving rise to a total of 36 evolved *P. aeruginosa* populations (18 S1 +18 S2), isolated from the 10-day partition communities.

Table 3: Summary of partition communities (biological replicates S1 and S2) containing independently evolved populations.

Community ID (R=richness level, C=combination)	**Species Identity** (used when picking out individual species)	
R1C1	A	
R1C2	B	
R1C3	C	P1 + P2
R1C4	D	
R1C5	E	
R1C6	F	
R2C1	AE	
R2C2	BC	
R2C3	DF	P1
R3C1	BCD	
R3C2	AFE	
R2C2	AD	
R2C3	BF	
R2C4	CE	P2
R3C3	ABC	
R3C4	DEF	
R6C1	A,B,C,D,E,F (A-F)	P1 + P2
PAO1	PAO evolved alone	P1 + P2
Ancestor	*PAO1 unevolved stock*	

2.5 Experiments in CF-mimicking sputum media

To test growth of *P. aeruginosa* in response to community context in a CF-like environment, Artificial Sputum Media (ASM) was prepared and used.

2.5.1 ASM Preparation

The ASM was prepared following the protocol of Kirchner *et al.*[75]. ASM contains type II mucin from porcine stomach, DNA from fish sperm, he iron-chelator diethylene triamine pentaacetic acid (DTPA), NaCl, KCl, KOH, egg yolk emulsion, and all essential and non-essential L-amino acids, all at concentrations found in an average pwCF. All ASM ingredients were purchased from Sigma-Aldrich. Briefly, 4g DNA was added slowly to 250ml of sterile water, and 5g mucin was dissolved in a further 250ml of sterile water. 0.25g of each amino acid (except cysteine and tyrosine) was dissolved in 100ml sterile water. Cysteine (0.25g) was dissolved in 25ml water and tyrosine (0.25g) was dissolved in 25ml of 0.5M KOH. In a further 100ml of sterile water, 5.9g DTPA, 5g NaCl, and 2.2g KCl were dissolved. The DNA, mucin, amino acids, and 5ml egg yolk emulsion were combined, and the pH was adjusted to pH 6.9 using 1M Tris-HCL. The solution was made up to a total volume of 1L with sterile water. The

ASM was then filter-sterilised using vacuum pump (brand) and Millipore Steritop filter units with a pore size of 0.22μm and neck size of 45mm.

2.5.2 Growth in ASM

A simple co-culture experiment was set up to test *P. aeruginosa* growth in ASM with respect to community context. We tested PAO1 and LESB58 to compare how the naïve vs CF-adapted strain would fare in a CF-mimicking environment in the presence/absence of the background community members. Overnight cultures of PAO1, LESB58, and the six species were diluted in ASM to an OD_{600} of 0.05 (~$1x10^7$ cells). Fourteen 30-mL glass universals containing 10mL ASM were set up as shown in Table 3. Diluted PAO1 and LESB58 cultures were inoculated into universals as monocultures (200μL), and with each of the background species (100μL + 100μL). ASM cultures were incubated at 37°C for 48 hours, shaking at 65rpm.

To dissolve the biofilm after 4 days of growth, a full sputasol vial (7.5ml) was mixed with 92.5ml sterile ddH_2O. 10mL of this was added to universals containing 10mL ASM (1:1) to disrupt the biofilm. The ASM cultures were then incubated for 30 minutes at 37°C, shaking at 200rpm. *P. aeruginosa* (PAO1 and LESB58) was isolated as mentioned previously. Briefly, 20μL of each culture was added to 180μL of PBS. Cultures were serially diluted 1:10 in and 10μL of each dilution (-1 to -8) was spotted onto square plates of C-N agar. The plates were incubated for 18 hours at 37°C, and the following morning CFUs were calculated *via* counting colonies at the higher dilutions. The ASM experiment was repeated independently three times to give three biological replicates.

Table 4: ASM experiment set up. Fourteen 30mL glass universals containing 10mL ASM were inoculated as follows;

PAO1 (PA) 200μL	PA + CA 100+100μL	PA + SA 100+100μL	PA + SH 100+100μL	PA + SE 100+100μL	PA + RD 100+100μL	PA + RM 100+100μL
LESB58 200μL	LES + CA 100+100μL	LES + SA 100+100μL	LES + SH 100+100μL	LES + SE 100+100μL	LES + RD 100+100μL	LES + RM 100+100μL

2.6 Statistical Analysis

2.6.1 Partition experiments

(i) Short-term

Linear models in RStudio (2023.06.2+561) were used to quantify the effect of each background community species on PAO1 final densities (CFU/ml) by using two separate linear models to partition

the variance between community richness and species identity. The species coefficients provided by this method give a measure of the effect of each species on the focal strain final densities relative to an average species. PAO1 final densities were averaged across two technical replicates per community (i.e. two replicates within the same 96-well plate). Natural log-transformed PAO1 densities were assigned as the response variable and richness as a factorial explanatory factor as follows:

Model 1: log(y) ~ richness

To assess the effect of species composition on PAO1 final densities, each species (A-F) was individually fitted as a factor to a new model containing only the residuals of model 1. This identified how much variance in the model was explained by (a) richness, and (b) species composition. Model validation to confirm that the model complied with assumptions of normality was performed by plotting the residuals versus fitted values [76].

Model 2: resid(Model 1)~-1+A+B+C+D+E+F

In order to test whether PAO1 grown in communities at each richness level differed significantly from PAO1 growth in isolation (i.e. red dash line in Fig.3A, 3B), Wilcoxon rank-sum one-sided t-tests were used, comparing PAO1 growth at each richness level against PAO1 growth alone; 25.9 (log $18x10^{10}$ i.e. red dashed line in Fig. 3A, 3B), quantified as the mean value of two technical replicates and three biological replicates.

(ii) Long-term

Densities of PAO1 after the 10-day passage experiment were quantified, and linear models were used in the same way as the short-term experiment to partition the variance between species richness and composition. Wilcoxon rank-sum tests were used as before to test whether PAO1 grown in communities at each richness level differed significantly from PAO1 growth in isolation; 31.19 (log $3.5x10^{13}$ i.e. red dashed line in Fig. 3A, 3B), quantified as the mean value of two biological replicates.

2.6.2 Phenotypic assays on evolved populations

All phenotypic assays were carried out independently at least three times for each of the S1 and S2 populations and relevant control/mutant strains. Production values were averaged across 3 technical replicates for each population, which was itself replicated 3 times. Hence, each evolved population had three biological replicates per assay.

Pyocyanin and pyoverdine results were analysed using the Bell model similar to the short and long-term partition experiments (2.6.2). Instead of quantifying the effect of background communities on PAO1 final densities, we looked at the effect of the communities on PAO1 pyocyanin and pyoverdine production (OD values).

To test whether evolved PAO1 populations isolated from communities at each richness level differed significantly from the PAO1 ancestor (i.e. black dash line in Fig.5A), Wilcoxon rank-sum one-sided t-tests were used, comparing PAO1 pyocyanin or pyoverdine production at each richness level against the ancestor.

Normality of each data set was tested for using residuals vs fitted values, Q-Q plots, and histograms.

To compare the means of each community with the means of the ancestor and evolved PAO1, Kruskal-Wallis rank sum was used with subsequent post hoc Dunn's tests with Bonferroni adjustment to evaluate differences between communities and the ancestor. These analyses were performed using the 'dunn.test' package.

3. RESULTS

3.1 Testing the effect of background community supernatant on *P. aeruginosa* growth.

To examine the effect of the secretomes of individual background community strains on PAO1, growth experiments with cell-free supernatants were performed. PAO1 was grown individually with the supernatants of each of the background species overnight. A growth inhibiting effect by supernatants from *C. albicans*, *R. dentocariosa*, *S. aureus*, *S. hominis*, and in part, *S. epidermidis*, with the strongest effect from *C. albicans*, where final OD600 is ~0.5, while PAO1 grown alone reaches a final OD of ~1.6 (**Fig.2).** The supernatants of the three staphylococci species all resulted in *P. aeruginosa* having a shorter, premature exponential phase, with *S. aureus* and *S. hominis* reducing growth rates and final OD greatly. *S. epidermidis* supernatant caused PAO1 to enter an earlier, shorter exponential phase and diauxic growth is observed. After a 10-hour lag period, a second growth phase is observed, and final OD is comparable to the wildtype. Diauxic growth is not seen for the other *Staphylococcus* strains, where stationary phase is after ~4-6 hours, and the final OD is ~1. Similar growth rates are seen when PAO1 is grown alone, or with *R. mucilaginosa* supernatant with the latter having a slightly higher final OD. As this experiment was done in duplicate, no statistical tests were performed.

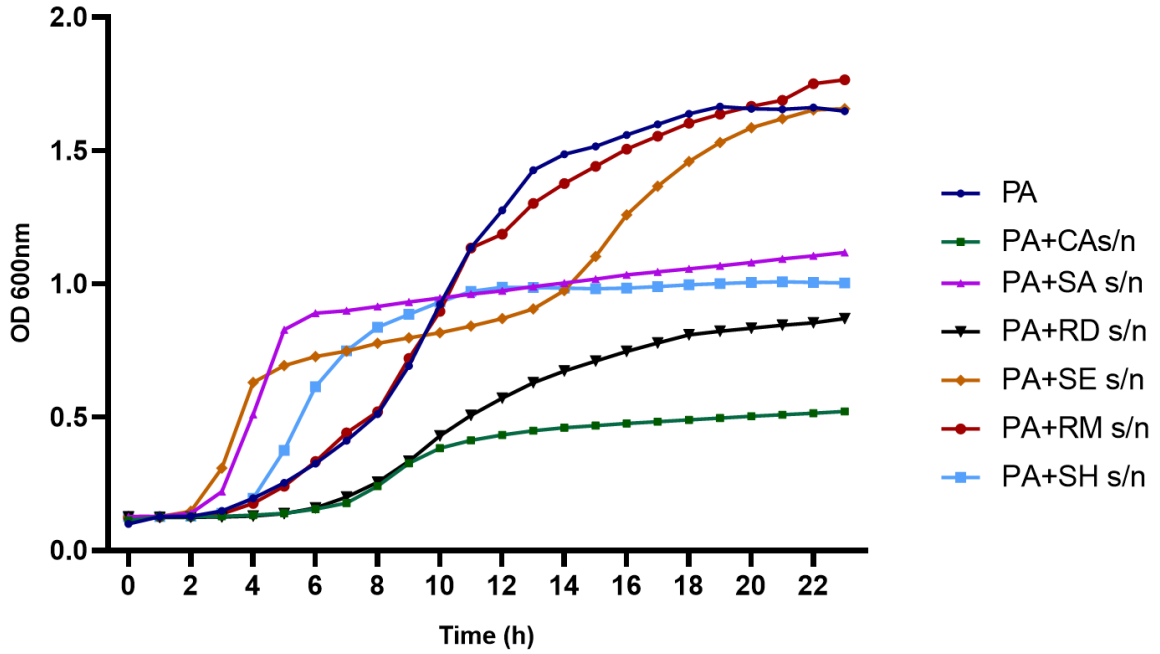

Fig. 2. Growth of *P. aeruginosa* PAO1 alone (PA), and with supernatants (s/n) of the six background species. CA; *C. albicans*, SA; *S. aureus*, RD; *R. dentocariosa*, SE; *S. epidermidis*, RM; *R. mucilaginosa*, SH; *S. hominis.* Data points represent the mean of two biological replicates.

3.2 Short-term Random Partition Model: How do background microbial community richness and composition impact *P. aeruginosa* final densities after 20 hours?

We first investigated how community context (species richness and composition) impacts final cell densities of PAO1 after 20 hours of growth. Synthetic communities were established varying in both richness levels and species composition using the random partition design established by Bell *et. al,* (2009).

3.2.1 Richness levels alone do not have a significant effect on PAO1 densities after 20 hours growth.

There was no significant effect of community richness on PAO1 final densities (Linear model, effect of richness; F = 0.7342, DF = 3,27, p=0.5369), suggesting species richness, or at least richness alone, does not affect PAO1 final densities significantly, explaining just ~4% of the variation in the linear model. PAO1 final densities were significantly inhibited by the presence of background community species, when grown in the presence of 1, 2, or 3 species (Wilcoxon rank-sum one sided t-test; R=1, p=0.0001, V=171; R=2, p=0.0001, V=171; R=3, p=0.001, V=78; **Fig. 3A, 3B**; PAO1 growth vs value of red dashed line), but were not significantly reduced when cultured in the presence of all 6 species, (Wilcoxon rank-sum one sided t-test; R=6, p=0.19, V=3; **Fig. 3A, 3B**; PAO1 growth vs value of red dashed line). However, it should be noted that sample size for this statistical test varies between richness levels (i.e. R = 2 contains datapoints for 3 communities (3 biological replicates each), while R = 6 contains datapoints for three biological replicates only, due to there being only one community of richness level 6, still resulting in full biological replicates for each community but graphed based on richness levels).

3.2.2 Species composition is an important predictor of PAO1 densities after 20 hours growth.

While species richness had poor explanatory power in the linear model (explaining just 4% of the variation in the model), species composition did significantly affect PAO1 final densities, explaining ~82% of the variation (Linear model, effect of species composition; F = 34.56, DF = 6,45, p<0.0001). When testing the effects of individual species, the model allows us to pinpoint species increasing or decreasing final PAO1 densities relative to an average species. Linear model coefficients (**Fig. 4A**.) for each species show the relative importance of a particular species for PAO1 final densities relative to the average of all species. Our model identified two species, *C. albicans* (species A) and *R. mucilaginosa* (species F), that were both associated with higher final PAO1 densities than the average species ($p < 0.001$ for both species) over the course of multiple partitions and individual experiments. Conversely, two species, *S. hominis* (species C; $p < 0.001$) and to a lesser extent, *S. epidermidis* (species D; $p < 0.05$), were associated with significantly decreased final densities of PAO1, relative to an average species. PAO1 grown in single-species communities with either *R. mucilaginosa* or *C. albicans* had the

highest final densities, while *S. hominis* and *S. epidermidis* had the lowest final densities. This suggests that, at least in this experimental setup, one-species communities were sufficient to predict dynamics of more diverse communities.

A

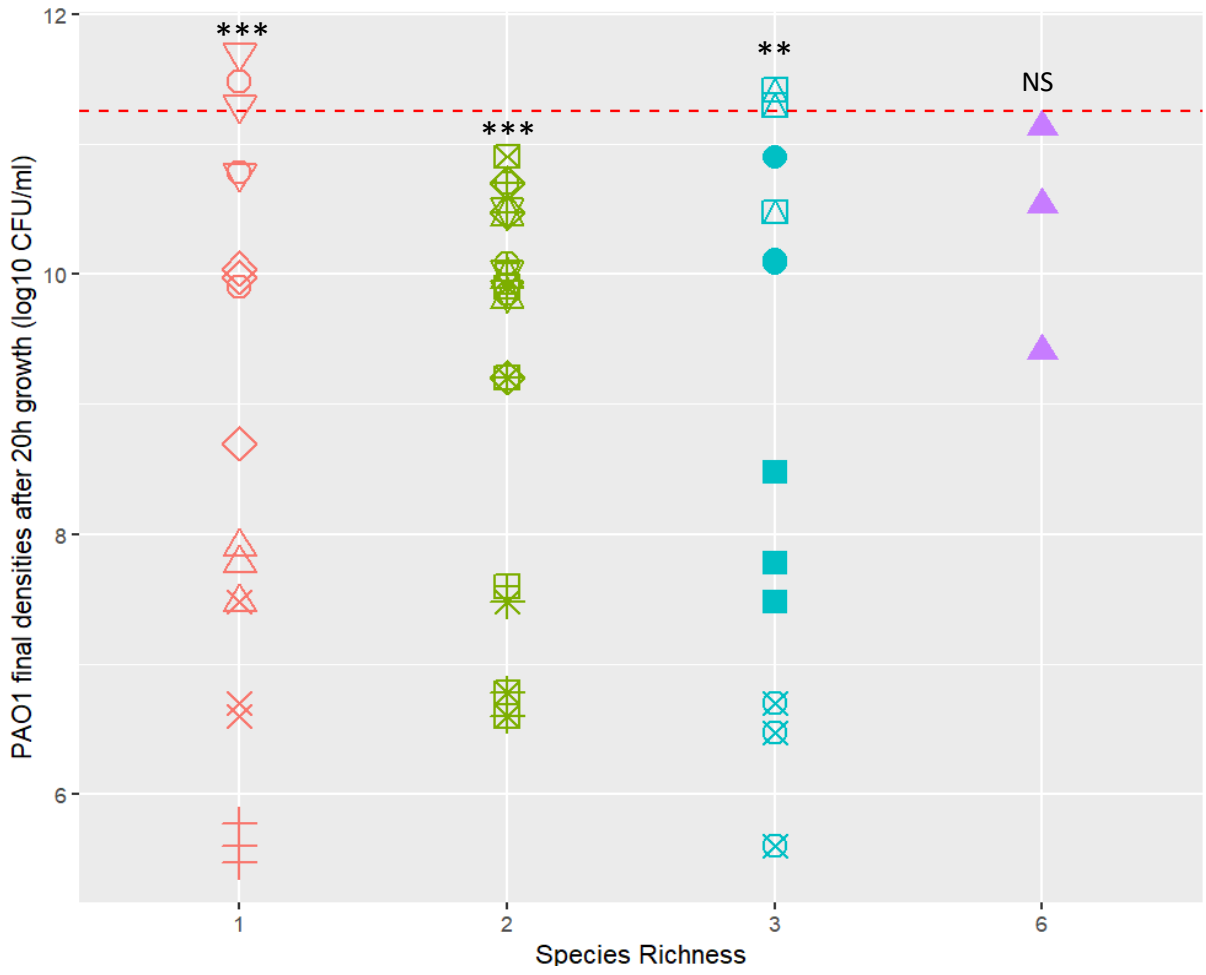

Fig. 3. (A) Final densities (log10(CFU/mL)) of PAO1 after 20 hours growth in communities of increasing richness levels 1, 2, 3, and 6, where a species richness refers to the number of species in the community other than PAO1. Red dashed line indicates the final mean density of *P. aeruginosa* grown alone, i.e. in a species richness of 0. Asterisks indicate that PAO1 densities at each richness level are significantly different from this red line (i.e. PAO1 densities are inhibited in communities relative to growth alone) Wilcoxon rank-sum tests, (*p <0.05, **p <0.01, ***p<0.001). Data from three independent experiments shown (experiments performed in three different weeks). **(B)** The data from **(A)** are shown as boxplots for individual communities, where interquartile range is represented by the median of three independent biological replicates for each community (Community ID), where R1=richness 1, R2=richness 2, etc; and C1=combination 1, C2=combination 2, etc.

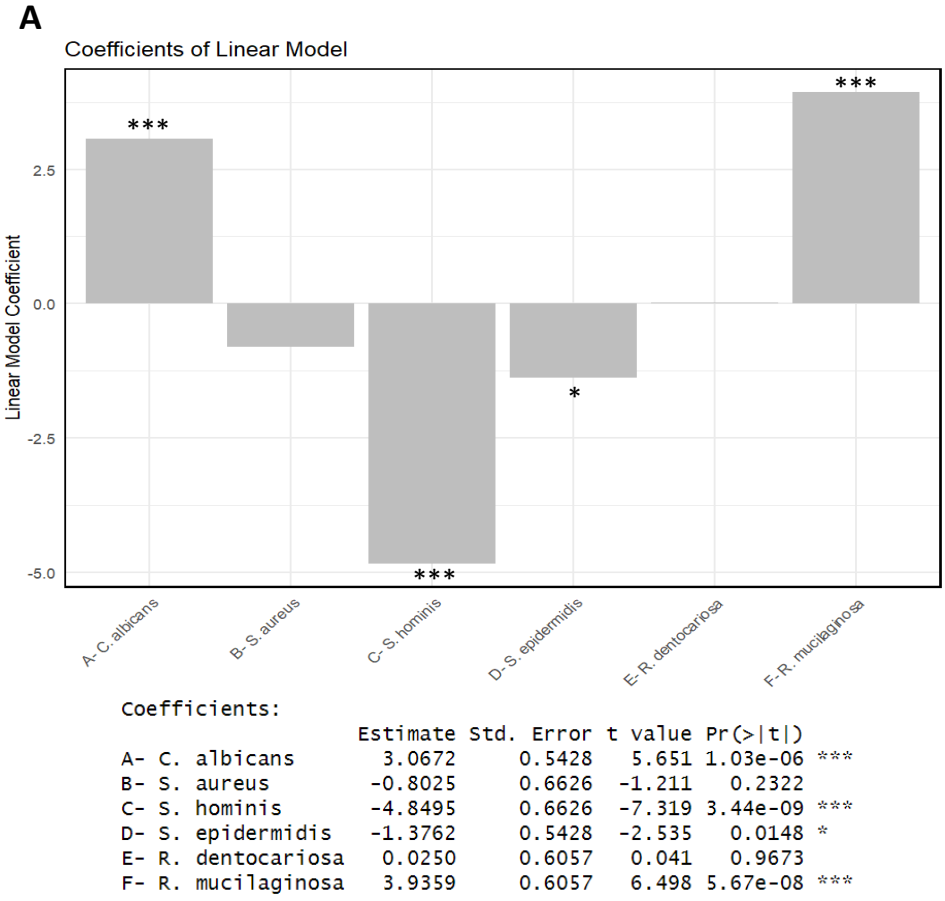

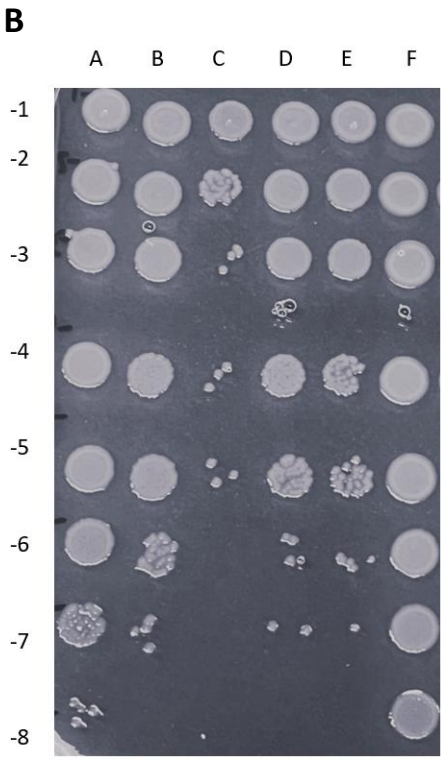

Fig. 4. (**A)** Linear model coefficients depicting positive and negative effects of species A – F on growth of *P. aeruginosa*. Species A (*C. albicans)* and F *(R. mucilaginosa)* were found to significantly increase final densities of *P. aeruginosa* relative to other species in the community, while species C *(S. hominis)* and to a lesser extent species D *(S. epidermidis)* significantly decreased final densities. * $p < 0.05$, ** $p < 0.01$, *** $p < 0.001$. Negative linear model coefficients suggest an overall negative effect of that species relative to the average species (species C and D), whereas positive values (species A and F) indicate a positive or promoting effect relative to the average species in the model. **(B)** Enumeration of PAO1 CFUs by spot-plating. PAO1 from communities (R=1) with species A-F was serially diluted and spotted onto Pseudomonas isolation agar supplemented with C-N. Each strain except F reduces CFU, with the strongest reduction seen in C (*S. hominis*) at $3x10^7$ CFU/ml. A-F denotes the species, -1 to -8 denotes dilution factor 10^1 to 10^8. Image is representative of three independent experiments.

3.3 Random Partition Model: The impact of community richness and composition on *P. aeruginosa* densities and the evolution of clinically relevant phenotypes after a 10-day passage experiment

Experiment (3.2) tested whether background species composition and richness affected PAO1 final densities after 20 hours growth. Next, the experiment was extended to a longer (10-day) timescale,

which would allow PAO1 to undergo evolutionary changes in response to either different richness levels or specific species.

3.3.1 Effect of community richness and composition on *P. aeruginosa* densities after a 10- day passage experiment

The same linear model approach described above was used to test how richness and composition affected PAO1 densities after a 10-day passage experiment, with the same set of communities described in methods 2.3. Consistent with previous results after 20h growth, there was no significant effect of community richness on PAO1 final densities after the 10-day passage experiment (Linear model, NS effect of richness; F = 1.863, DF = 3,30, p = 0.16), with richness explaining just 16% of model variance. However, in stark contrast to the 20h short-term experiment, the 10-day experiment found that PAO1 final densities were increased by the presence of background community species, when grown in the presence of 1, 2, or 3 species, relative to PAO1 densities when passaged alone (Wilcoxon rank-sum one-sided t-test; R=1, p=0.0013, V=78; R=2, p=0.0013, V=78; R=3, p=0.007, V=36 ; **Fig. 5A, 5B**; PAO1 growth vs value of red dashed line). Consistent with the short-term 20h experiment, no significant effect of growing in a 6-species community was observed relative to PAO1 growing alone (Wilcoxon rank-sum one-sided t-test; R=6, p=0.19, V=3; **Fig. 5A, 5B**; PAO1 growth vs value of red dashed line), although this is likely due to an n=2 biological replicates in this particular richness category as there is only one possible combination of richness level 6.

Next, we tested whether community composition significantly affected PAO1 densities after the 10-day passage experiment, by fitting "composition" to the residuals of the species richness linear model. In contrast to the 20h short-term experiment, the 10-day passage experiment showed that PAO1 densities were not affected by species composition – composition explained just 7% of the variation in the model (Linear model, effect of composition; F = 0.3776, DF = 6,28, p = 0.0887). No species were identified that were associated with increased or reduced PAO1 densities, relative to an average species ($p > 0.05$ for all species, **Fig. 6**). Hence, while the short term 20h experiment saw significant growth inhibiting effects of *S. hominis* and positive effects of *R. mucilaginosa* and *C. albicans*, extending the timeframe of the experiments negated these effects. While not significant statistically, we observe *S. aureus* trending towards a positive effect on *P. aeruginosa* final densities (**Fig. 6A**), and this was visualised in the spot plating (**Fig.6B**), showing *S. aureus* provided the least competition and/or inhibitory effects which suggests to some form of coexistence or mutual interaction occurring [45].

A

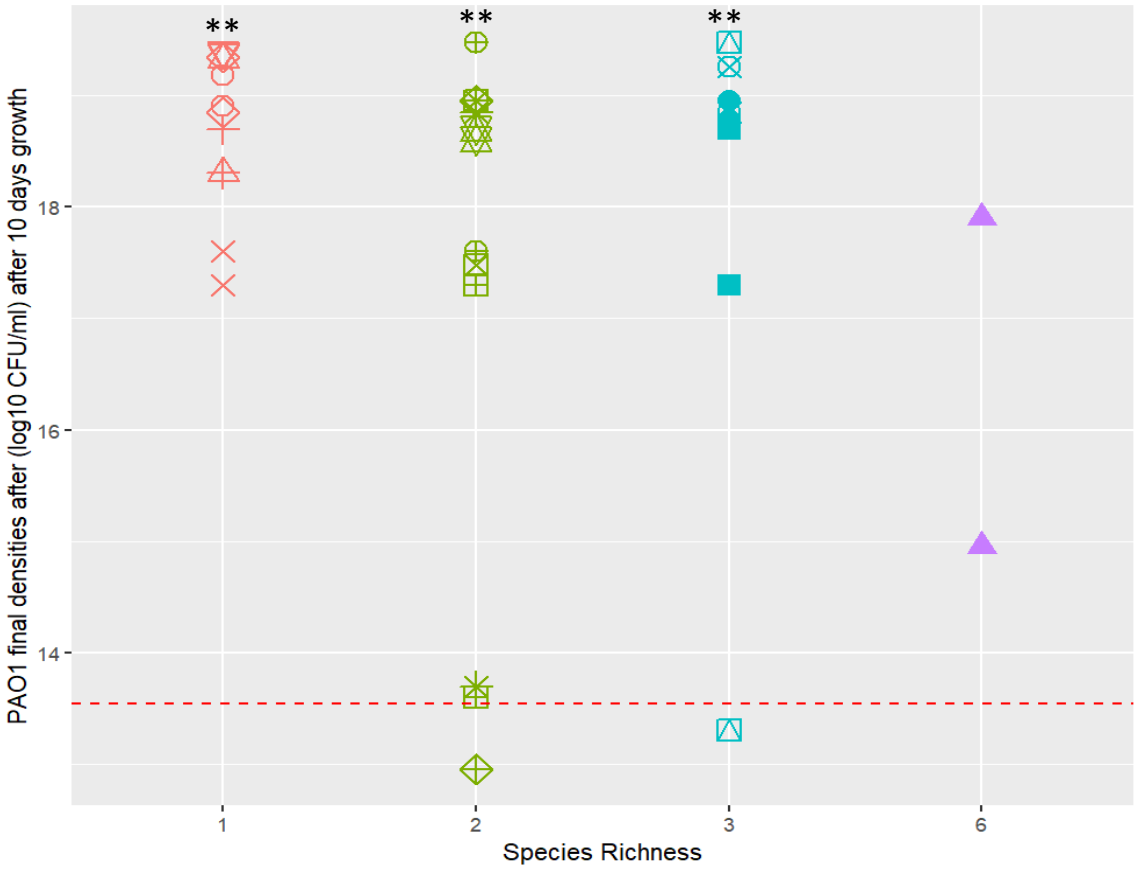
**
**
**
18
16
14
PAO1 final densities after (log10 CFU/ml) after 10 days growth
1
2
3
6
Species Richness

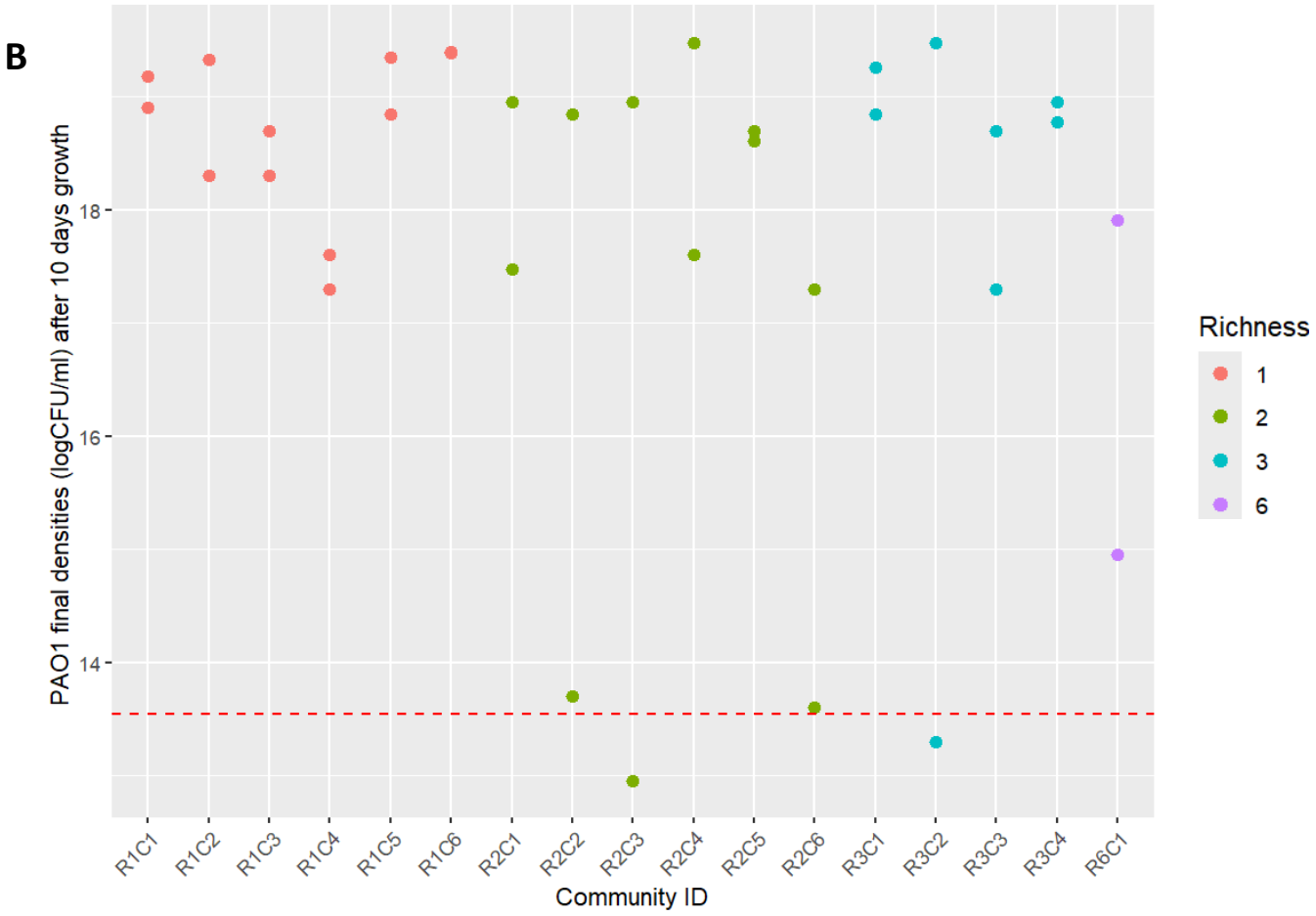

Fig. 5. (A) Final densities (log(CFU/mL)) of PAO1 after 10 days of growth in communities of increasing richness levels 1, 2, 3, and 6, where a species richness of 3 indicates there are 3 species other than PAO1. Individual community IDs are also shown. Biological replicates (n=2) for each PAO1 population are depicted as different shapes. Red dashed line indicates the final mean density of *P. aeruginosa* passaged i.e. in a species richness of 0. Asterisks indicate that PAO1 densities at each richness level are significantly different from this red line (i.e. PAO1 densities are increased in communities relative to growth alone), Wilcoxon rank-sum tests, (*p <0.05, **p <0.01, ***p<0.001). **(B)** The same data from **(A)** are shown for individual PAO1 populations (Community ID).

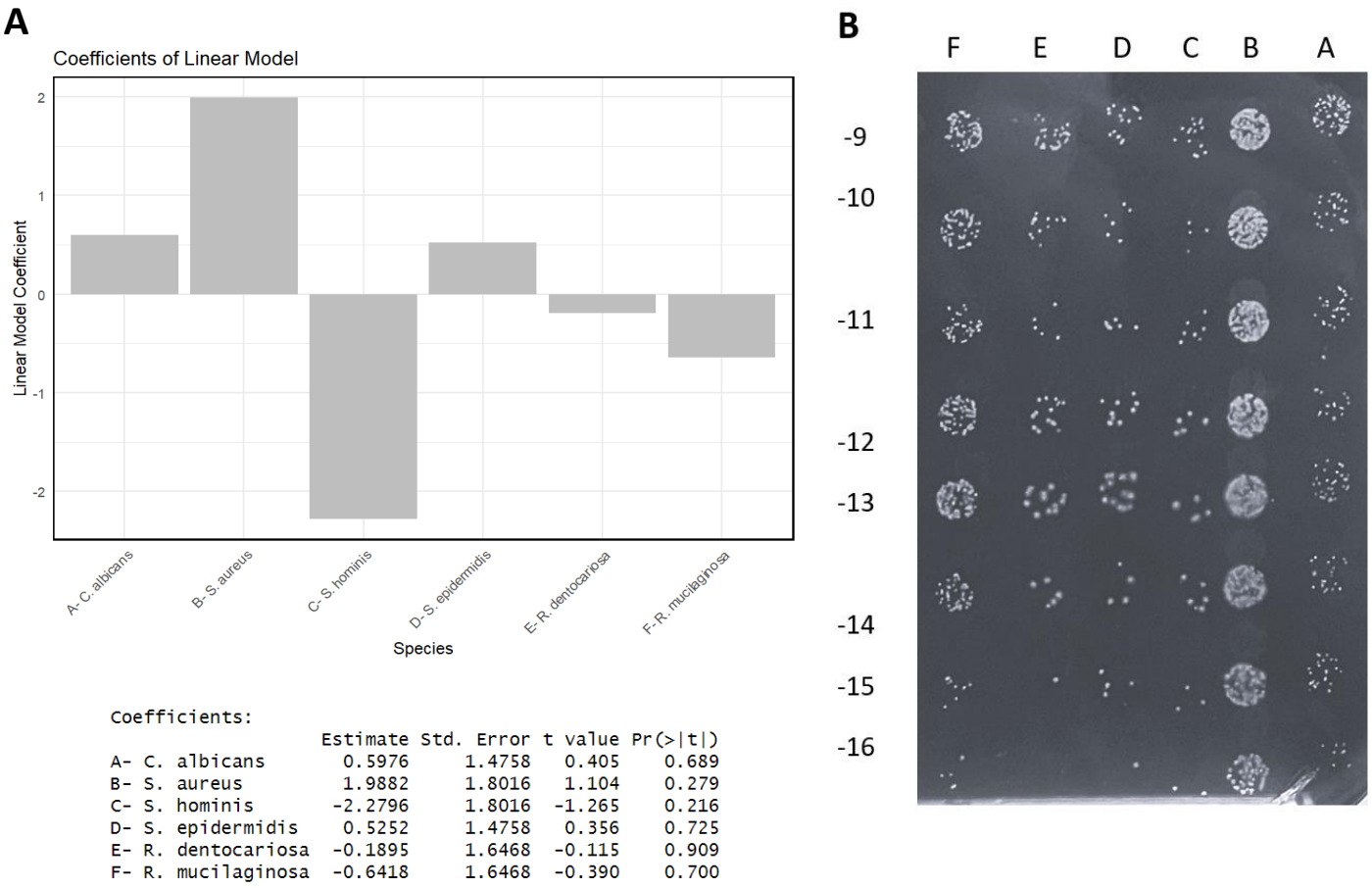

Coefficients:

	Estimate	Std. Error	t value	Pr(>|t|)
A- C. albicans	0.5976	1.4758	0.405	0.689
B- S. aureus	1.9882	1.8016	1.104	0.279
C- S. hominis	-2.2796	1.8016	-1.265	0.216
D- S. epidermidis	0.5252	1.4758	0.356	0.725
E- R. dentocariosa	-0.1895	1.6468	-0.115	0.909
F- R. mucilaginosa	-0.6418	1.6468	-0.390	0.700

Fig. 6. (**A)** Linear model coefficients depicting positive and negative effects of species A – F on growth densities of *P. aeruginosa* PAO1 after a 10-day passage experiment. No species were identified that had significant impacts on PAO1 densities relative to an average species. Negative linear model coefficients suggest an overall negative effect of that species relative to the average species, whereas positive values indicate a positive effect relative to the average species in the model. While species C shows some inhibition of PAO1 densities, and species B shows some promotion of PAO1 densities, these results were not statistically significant. **(B)** Enumeration of PAO1 CFUs by spot-plating. PAO1 from communities (R=1) with species A-F was serially diluted and spotted onto Pseudomonas isolation agar supplemented with C-N. A-F denotes the species, -1 to -8 denotes dilution factor 10^1 to 10^8. Image is representative of three independent experiments.

3.3.2 Quantifying clinically-relevant changes in "evolved" *P. aeruginosa*

After the extended 10-day partition experiment, day 10 populations were isolated from each partition community (see methods section 2.4.2). Phenotypic analyses were performed on PAO1 populations isolated from the background communities. This was to quantify that the changes observed during the experiment, such as colour and viscosity, were retained when PAO1 populations were isolated, and not just a direct short-term response that occurs only in the presence of other species. Phenotypes examined were production of virulence factors (pyocyanin and pyoverdine), antibiotic susceptibility, biofilm formation and colony morphology.

3.3.2.1 Pyocyanin production

Production of pyocyanin by PAO1 evolved populations was measured to test the impact of community context on this clinically relevant phenotype. Due to the interesting and unique evolutionary trajectories of the corresponding biological replicate pairs, we did not pool the replicates but instead treated the two replicates for each community as independently evolved populations of PAO1. For ease, the first set of biological replicates will be referred to as Set 1or S1 and the second as Set 2 or S2, i.e., there is an R1C1 from set 1 and set 2 as each has varying pyocyanin production.

While species richness did not have an effect on PAO1 final densities in the short-term and 10-day partition experiments, species richness did affect PAO1 pyocyanin production overall in both set 1; (Linear model, effect of richness; F=11.11, DF=4, 49, $p < 0.001$), explaining 40% of model variation, and set 2; (Linear model, effect of richness; F=4.609, DF=4, 55, $p < 0.01$(p=0.00279)), explaining 20% of model variation.

PAO1 pyocyanin production was increased by the presence of background community species, when grown in the presence of 2 or 3 species relative to the unevolved ancestor (S1=Wilcoxon rank-sum test ; R=2, $p < 0.001$, V=171; R=3, $p < 0.01$(0.0043), V=63; **Fig. 7A**; pyocyanin RFU vs value of black dashed line). No significant effect of growing in a 1- or 6-species community on pyocyanin production was observed relative to the pyocyanin production of the ancestor (S1=Wilcoxon rank-sum test; R=1, p=0.94, V=51; R=6, p=0.09, V=6; **Fig. 7A**; pyocyanin RFU vs value of black dashed line). The populations from set 1 (S1) displayed a similar richness-dependent effect where pyocyanin production was increased when PAO1 was evolved and isolated from 2- or 3-species communities, but not in the case of single-species, or 6-species communities (S2=Wilcoxon rank-sum test; R=1, p=0.16, V=109; R=2, p=0.0034, V=148; R=3, p=0.0053, V=72; R=6, p=0.09, V=6; **Fig. 7B**; pyocyanin RFU vs value of black dashed line). PAO1 from S1 evolved in isolation (R=0) displayed reduced pyocyanin production relative to the ancestor (One-sided t-test; Ancestor vs PAO1; p<0.05). Interestingly, PAO1

from S2 evolved alone did not show any significant change in pyocyanin production relative to the ancestor (One-sided t-test; Ancestor vs PAO1; p=0.79). This shows that two identical starting populations can undergo various "microevolutionary" changes, even in as short as a period of 10 days.

Species composition also had a significant effect on pyocyanin production, explaining 59% of the variation for S1 populations (Linear model, effect of species composition; F=11.49, DF=6,48, p <0.001), and 14% of the variation for S2 populations (Linear model, effect of species composition; F=2.57, DF=6,54, p <0.05). Linear model coefficients (**Fig. 9)** for each species show the relative importance of particular species for PAO1 pyocyanin production relative to the average of all species. Our model identified two species *C. albicans* (species A), and *R. dentocariosa* (species E), that negatively affect pyocyanin production (species A; p< 0.001, species E; p < 0.01). Hence, communities containing *C. albicans* and/or *R. dentocariosa* may be expected to inhibit pyocyanin production. *R. mucilaginosa* (species F) was associated with significantly high pyocyanin production (p < 0.001) suggesting that communities with this species may promote PAO1 pyocyanin production. Interestingly, we also found *R. mucilaginosa* to be positively affecting PAO1 final densities in the short-term partition experiment. It would be necessary in future to track the densities of the background community members, as in this case, this positive effect may be due to enhanced killing of *R. mucilaginosa* by *P. aeruginosa*, therefore resulting in low and high densities of *R. mucilaginosa* and *P. aeruginosa* respectively.

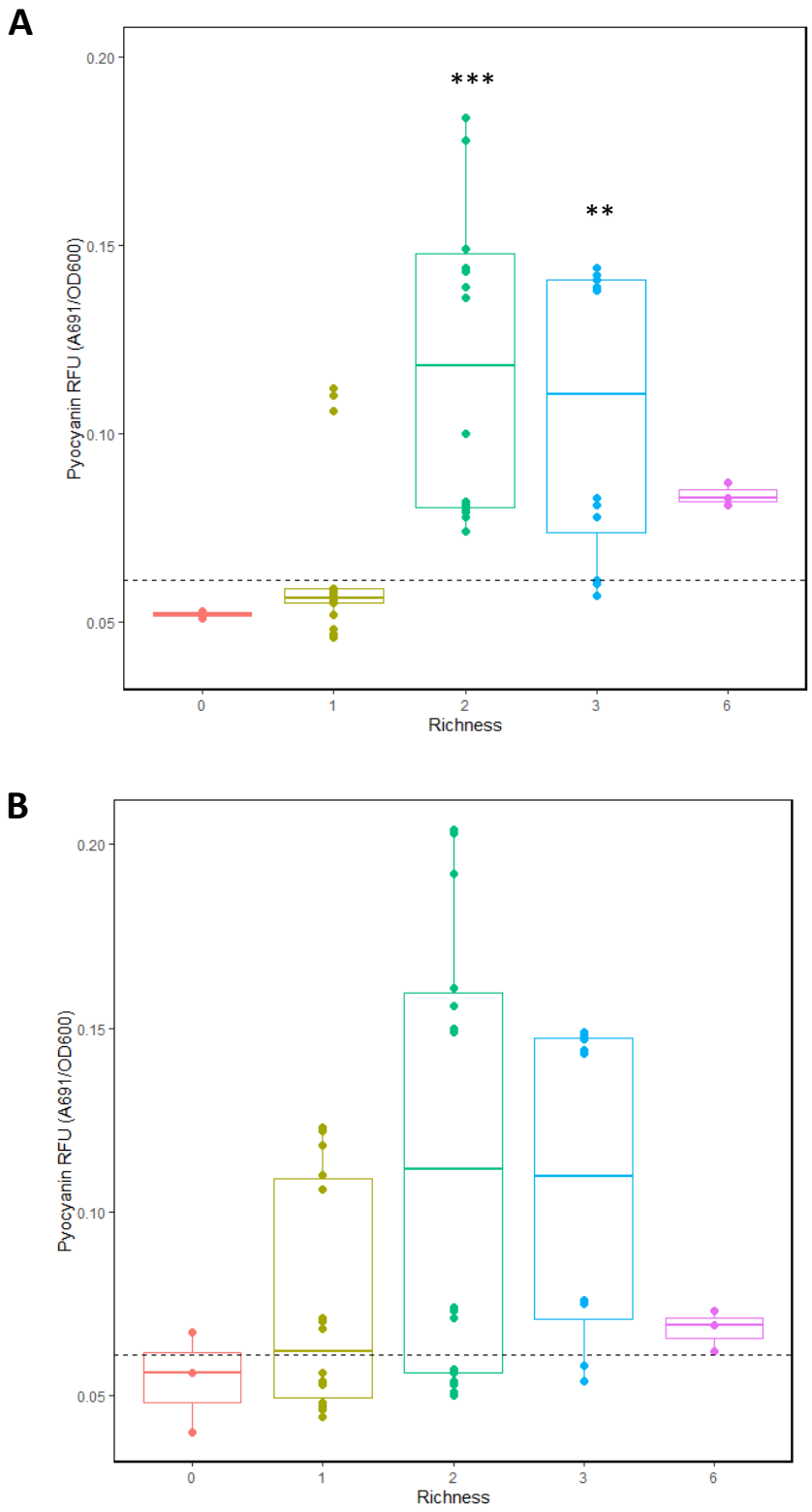

Fig. 7. *Per capita* pyocyanin production of S1 populations **(A),** and S2 populations **(B)**, after 24 hours of growth. Pyocyanin was quantified by measuring fluorescence of culture supernatants at A691 and standardising by OD600. This gave the RFU (relative fluorescence units). Each population in both sets, S1 and S2, were tested independently three times (3 biological replicates). Richness level of 0 represents the PAO1 population evolved without any background community. Richness level of 1 contains all the populations evolved from one-species communities, richness level 2 contains populations evolved from 2-species communities (three unique 2-species communities), and so forth. Black dashed line indicates the average pyocyanin production value of the unevolved PAO1 ancestor. Asterisks represent significance when comparing richness levels to the ancestor *via* Wilcoxon rank-sum tests, (*p <0.05, **p <0.01, ***p<0.001).

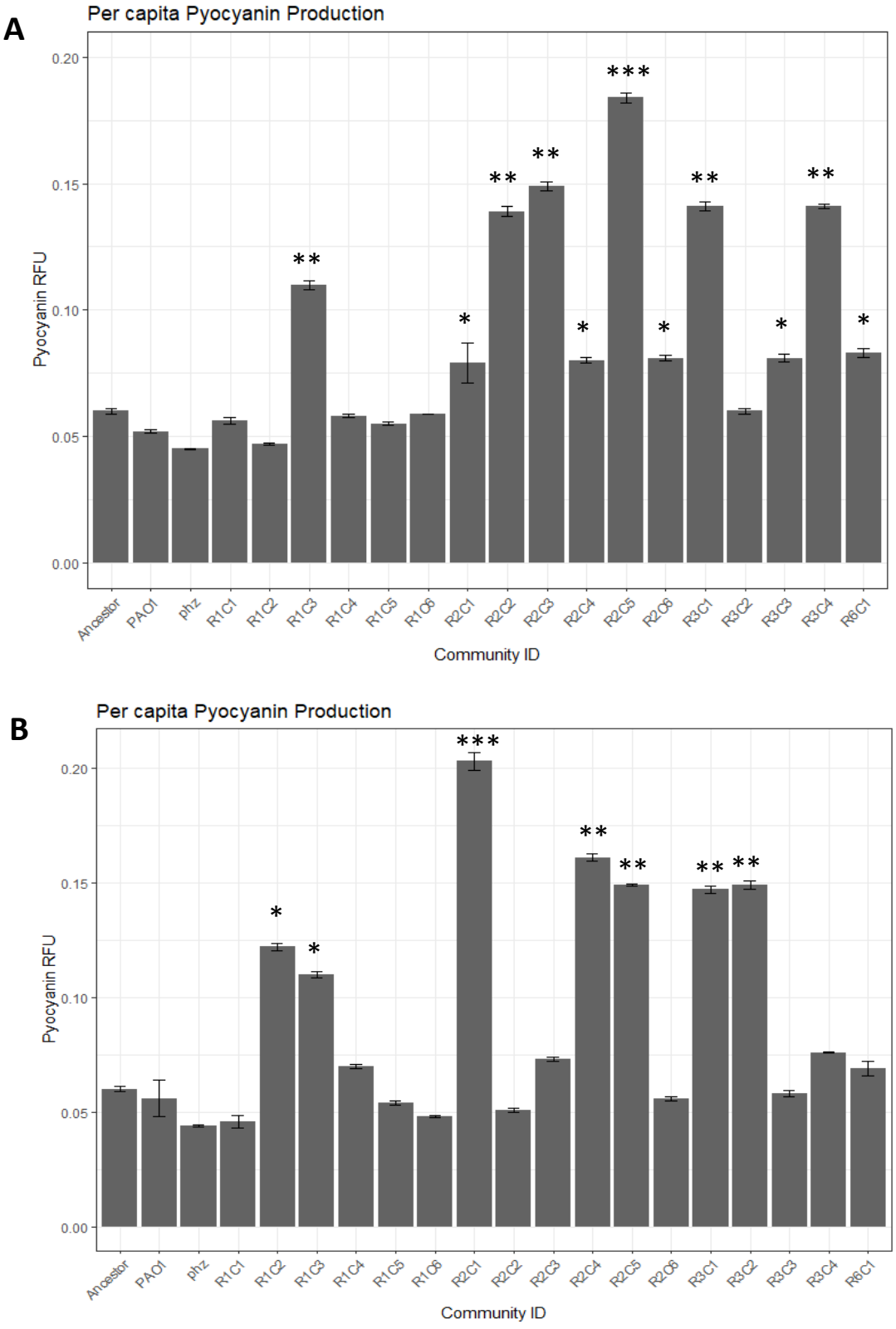

Fig. 8. *Per capita* pyocyanin production of S1 populations **(A),** and S2 populations **(B)**, after 24 hours. Pyocyanin production was quantified via measuring the supernatant of cultures at A691 and standardising by the OD600. This gave the RFU (relative fluorescence units). Each population in both sets, S1 and S2, were tested independently three times (3 biological replicates). Each bar represents the

mean of three biological replicates ±SD of each specific community in S1 and S2. The "Ancestor" refers to the original unevolved PAO1 strain (Black dashed line in **Fig. 7** and "PAO1" is the evolved population that was passaged without any community. The PAO1 phenazine deletion mutant (*Δphz*) was used as a negative control as it lacks the phenazine biosynthesis operon. Kruskal Wallis, with Dunn post hoc tests were used to test for statistical significance between means of the groups when compared to the ancestor and PAO1 alone. The comparisons against PAO1 alone ("PAO1" on graph) are denoted on the graph with asterisks representing significance (*p <0.05, **p <0.01, ***p<0.001).

A reminder that S1 ***(A)****, and S2* ***(B)*** *are composed of evolved biological replicates from the extended partition experiment that were treated as individual evolved populations for phenotypic analyses, i.e. R2C1 from S1 (set 1)* ***(A)****, and R2C1 from S2 (set 2)* ***(B)****, began as biological replicates in the extended partition experiment but PAO1 isolated from each them at the end were treated as two independently evolved populations despite having the same community composition. All phenotypic analyses carried out on each evolved population were always done three times independently.*

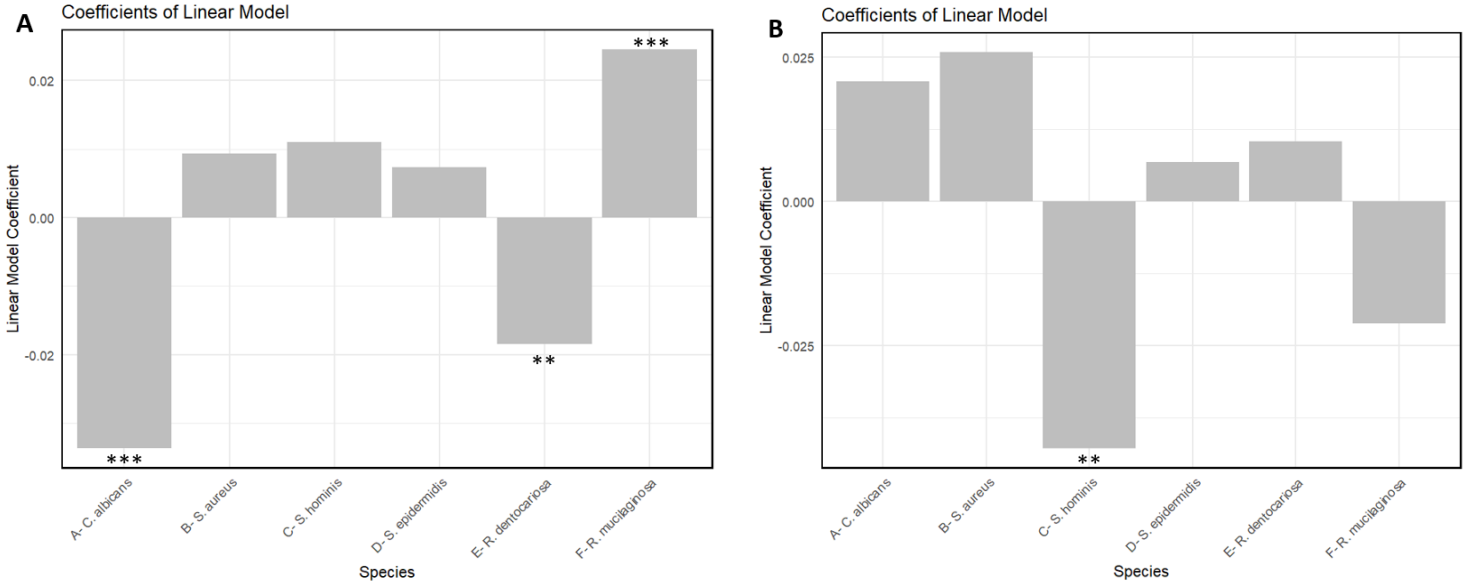

Fig. 9. Linear model coefficients depicting positive and negative effects of species A – F on pyocyanin production of PAO1 evolved populations from S1 **(A)** and S2 **(B)** population sets. Negative linear model coefficients suggest an overall negative effect of that species relative to the average species, whereas positive values indicate a positive effect relative to the average species in the model. When looking at S1 (set 1) **(A)**, species A, and E, *C. albicans* and *R. dentocariosa* respectively, were associated with lower *P. aeruginosa* pyocyanin production compared to average community species, whereas *R, mucilaginosa* (species F) was associated with increased pyocyanin production. For S2 (set 2) **(B)**, species C, *S. hominis* was associated with negatively affecting pyocyanin production relative to the average species. Species A and B displayed a positive trend but were not found to be statistically significant in positively affecting pyocyanin values. (*p <0.05, **p <0.01, ***p<0.001).

3.3.2.2 Loss of pyoverdine production is seen in S2 evolved populations of *P. aeruginosa* but not in S1.

The iron-scavenging siderophore pyoverdine was measured next using an excitation-emission assay. Unlike in the case of pyocyanin production, species richness did not have a significant effect on PAO1 pyoverdine production for either of the set 1 or set 2 populations (Linear model, effect of richness; S1: p=0.07; S2: p=0.81). When looking at each richness level individually, growing in the presence of 2-species communities had a significant effect on pyoverdine production (S1=Wilcoxon rank-sum test ; R=2, p = 0.013, V=28), while growing in the presence of 1-, 3-, or 6-species, had no significant effect on PAO1 production, (S1=Wilcoxon rank-sum test ; R=1, p = 0.36, V=64; R=3, p = 0.56, V=31; R=6, p = 0.18 V=0). Interestingly, for set 2, (S2 populations), there was a significant effect of growing in 1-, 2-, and 3-species communities, with PAO1 isolated from these richness levels displaying significantly decreased pyoverdine production; (S2=Wilcoxon rank-sum test ; R=1, p <0.001, V=4; R=2, p <0.001, V=0; R=3, p <0.01 V=1). Similarly to the S1 populations, there was so significant effect of growing in a 6-species community, (S2=Wilcoxon rank-sum test; R=6, p =0.18, V=0).

PAO1 from S1 evolved in isolation (R=0, **Fig. 10A**) showed no significant change in pyoverdine production relative to the ancestor (One-sided t-test; Ancestor vs PAO1; p=0.38). Interestingly, PAO1 from S2 evolved alone (R=0, **Fig. 10B**) displayed a significant decrease or loss in pyoverdine production relative to the ancestor (One-sided t-test; Ancestor vs PAO1; p<0.05). This once again shows how two identical starting populations can undergo various "microevolutionary" changes, even in as short as a period of 10 days, and this result is inverse to what was seen regarding the PAO1 evolved alone populations in terms of pyocyanin production compared to the ancestor.

There was overall no significant effect of species composition on pyoverdine production for S1 populations, (Linear model, effect of species composition; F=2.07, DF=6,54, p=0.07), or for S2 populations, (Linear model, effect of species composition; F=0.89, DF=6,54, p=0.51). However, when picking out the relative effects of individual species *via* linear model coefficients, we found that for S1 populations (**Fig. 12A)**, species E (*R. dentocariosa)* was negatively affecting pyoverdine production (p < 0.05), while species F (*R. mucilaginosa)* was found to be positively affecting pyoverdine production (p < 0.05). For S2 (**Fig. 12B),** species C (*S. hominis)* was associated with decreased pyoverdine production (p < 0.05). The trends seen here with *R. dentocariosa* and *R.mucilaginosa* were also observed in terms of pyocyanin production suggesting these species may play a role in directly or indirectly influencing the expression of these two putatively linked virulence factors. Each individual community for S1 and S2 populations was also compared to the ancestor and PAO1 evolved alone (**Fig. 11).**

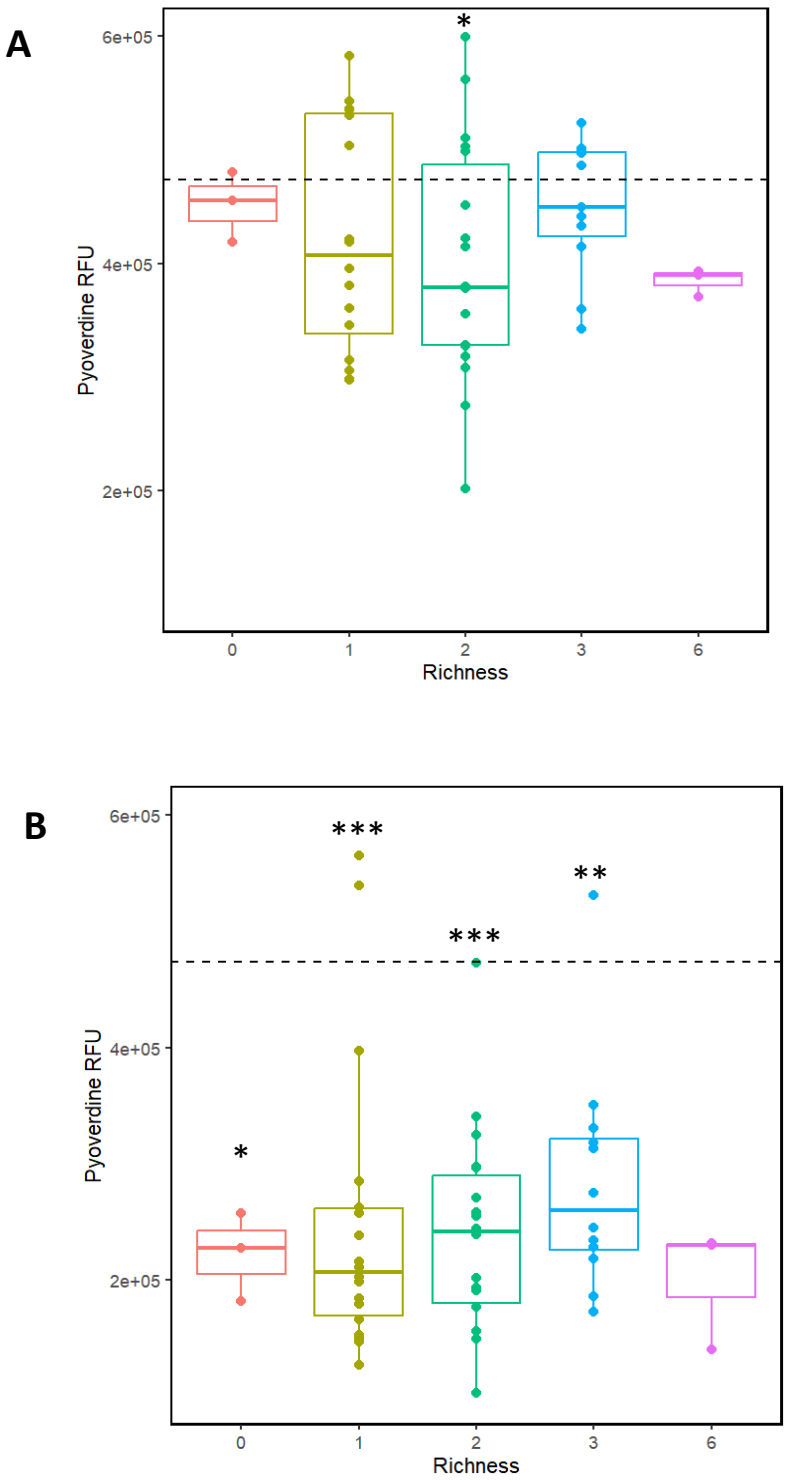

Fig. 10. *Per capita* pyoverdine production of S1 populations **(A),** and S2 populations **(B)**, after 24 hours of growth in iron-limited CAA media, graphed in terms of richness. A pyoverdine-specific excitation-emission assay was used to quantify production of the main siderophore in *P. aeruginosa*, pyoverdine. Evolved isolates were grown in LB, followed by overnight growth in CAA media made iron-limited by the addition of freshly prepared apo-transferrin and sodium bicarbonate. Pyoverdine production was quantified via measuring the fluorescence of cultures in CAA at 460nm following excitation at 400nm. The ratio fluorescence/OD600 was used to give a quantitative measure of *per capita* pyoverdine

production. This gave the RFU (relative fluorescence units). Each population in both sets, S1 and S2, were tested independently three times, and biological replicates are shown on the graphs with the boxplots representing the average of each richness level. Richness level of 0 represents the evolved PAO1 population without any background community. Richness level of 1 contains all the populations evolved from one-species communities, richness level 2 contains populations evolved from 2-species communities (three unique 2-species communities), and so forth. Black dashed line indicates pyoverdine production value of the unevolved PAO1 ancestor. Asterisks represent significance when comparing richness levels to the ancestor *via* Wilcoxon rank-sum tests, (*p <0.05, **p <0.01, ***p<0.001).

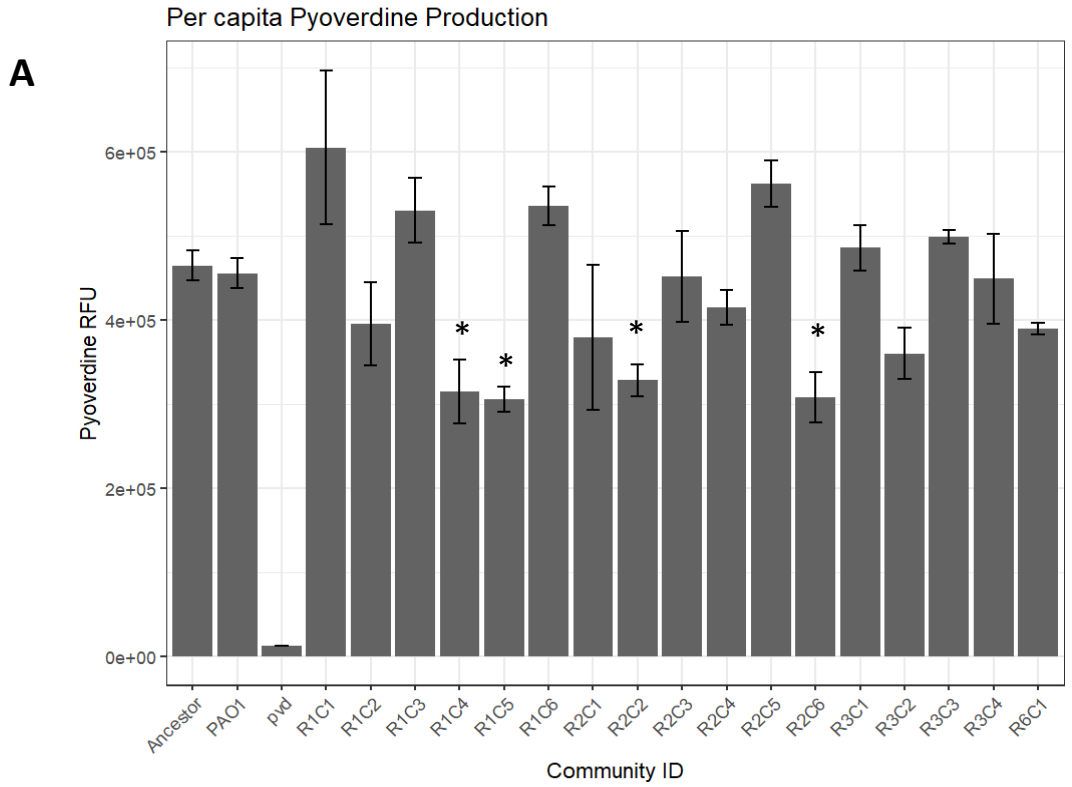

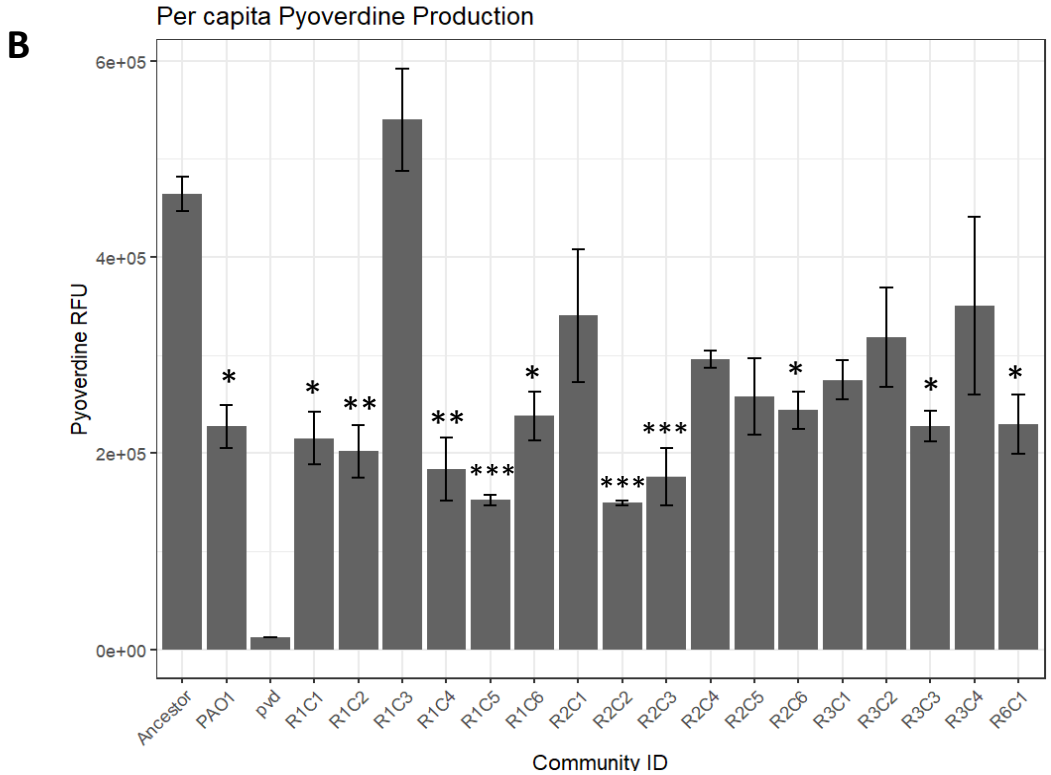

Fig. 11. *Per capita* pyoverdine production of S1 populations **(A),** and S2 populations **(B)**, after 24 hours of growth graphed in terms of community ID/composition. Pyoverdine production was quantified via measuring the fluorescence of cultures in CAA at 460nm following excitation at 400nm. The ratio fluorescence/OD600 was used to give a quantitative measure of *per capita* pyoverdine production. This gave the RFU (relative fluorescence units). Each population in both sets, S1 and S2, were tested using this assay in triplicate (3 technical replicates in 96-well plate) and independently three times (3 biological replicates). Each bar represents the mean of three biological replicates ±SD of each specific community in S1 and S2. The "Ancestor" refers to the original unevolved PAO1 strain (Black dashed line in **Fig. 9(A), (B)**) and "PAO1" is the evolved population that was passaged without any community. The PAO1 phenazine deletion mutant (Δpvd) was used as a negative control as it lacks the phenazine biosynthesis operon. Kruskal Wallis, with Dunn post hoc tests were used to test for statistical significance between means of the groups when compared to the ancestor and PAO1 alone. The comparisons against the ancestral strain are denoted on the graph with asterisks representing significance (**p* <0.05, ***p* <0.01, ****p*<0.001).

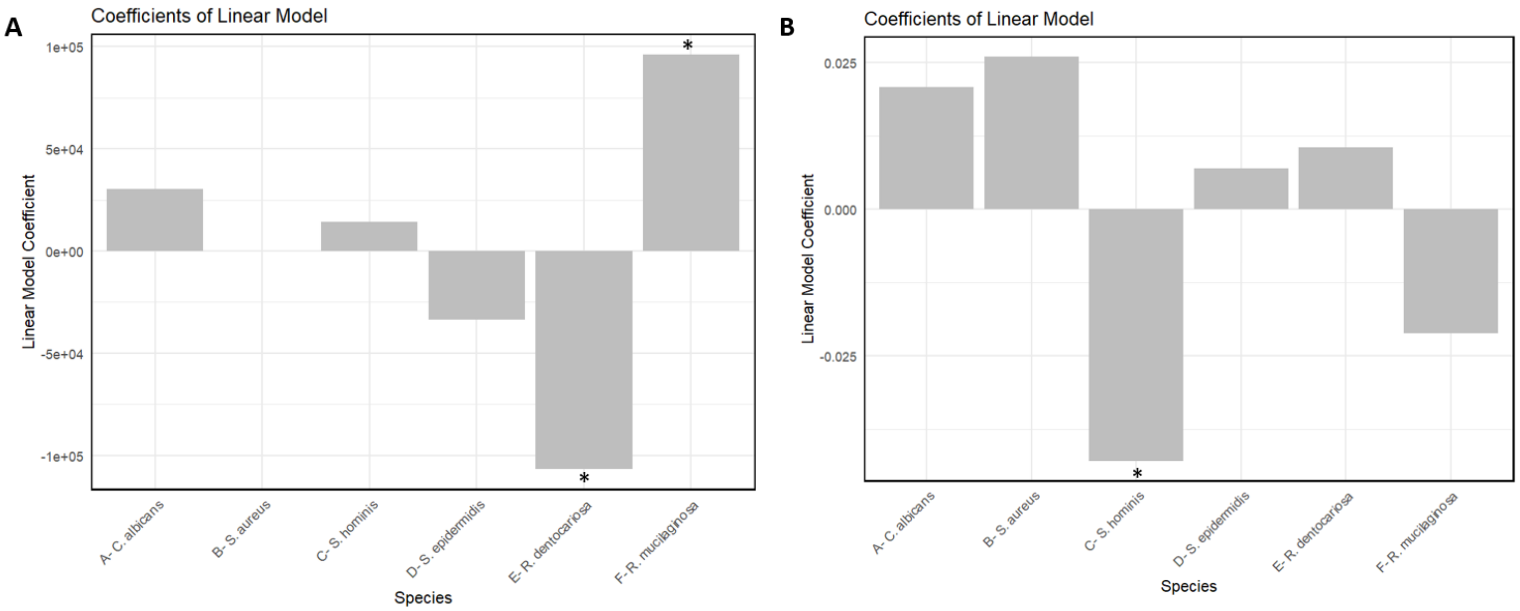

Fig. 12. Linear model coefficients depicting positive and negative effects of species A – F on pyoverdine production of PAO1 evolved populations from S1 **(A)** and S2 **(B)** population sets. Negative linear model coefficients suggest an overall negative effect of that species relative to the average species, whereas positive values indicate a positive effect relative to the average species in the model. When looking at S1 (set 1) **(A)**, species E, *R. dentocariosa* was negatively affecting pyoverdine production, relative to the average species, while species F, *R. mucilaginosa* was associated with increased pyoverdine production. For S2 (set 2) **(B)**, species C, *S. hominis* was associated with negatively affecting pyoverdine production relative to the average species. Species A and B displayed a positive trend but were not found to be statistically significant in positively affecting pyoverdine values. (**p* <0.05, ***p* <0.01, ****p*<0.001).

3.3.2.3 Community context alters the antibiotic susceptibility of *P. aeruginosa* and is linked to multispecies biofilm formation with key species.

To test the antibiotic susceptibility of the evolved PAO1 populations, we measured the Minimum Inhibitory Concentration (MIC) of colistin, a common last-resort antibiotic for *P. aeruginosa* infections. It was shown recently that bacteria evolving with *C. albicans* become phenotypically but not genotypically resistant to colistin, in response to magnesium ion competition [77]. Since many of our communities contain *C. albicans*, we wanted to test if a similar response was observed.

For the six communities where *C. albicans* was present, three contained colistin resistant *P. aeruginosa*. Interestingly, when *R. dentocariosa* was present alongside *C. albicans* (i.e. the remaining three communities), no colistin resistance was observed in *P. aeruginosa*. We also found that of the six communities containing *S. aureus*, four of them harboured colistin resistant *P. aeruginosa*.

The six species community did not affect colistin resistance, maybe due to all species being at lower relative abundances overall, so individual species have less of an effect. This would need to be confirmed by tracking densities of the background communities to compare abundances relative to *P. aeruginosa*, particularly in the higher richness levels where findings may be a result of differences in abundance, rather than composition having an effect.

No significant differences were observed in the resistomes of the populations tested for any of the antibiotics analysed. However, there were some isolated heterogeneous communities displaying meropenem tolerance/resistance within some of the populations containing species A, *C. albicans* and/or species B, *S. aureus.* These colonies were grown again and the meropenem disc assay was repeated. We found that two out of the five sub-population were resistance to meropenem, with the other three displaying intermediate resistance (**Fig. 13A, 13B)**. However, since this was only one passage, it is unknown whether this was due to a stable mutation or an amplification, or perhaps just passive resistance. This would need to be repeated with multiple passages to confirm whether this is a stable mutation for resistance and retained.

Table 5: Minimum inhibitory concentrations (MIC) of evolved *P. aeruginosa* populations and the partition community from which they were isolated. The microbroth dilution method was used to determine colistin resistance based on EUCAST breakpoints. *P. aeruginosa* isolated from communities with *C. albicans* or *S. aureus* showed resistance to colistin. The result is the mode of six biological replicates (S1 and S2 pooled). Asterisks indicate control results from ATCC strains.

			Colistin
Strain	**Community Isolated from**	**MIC**	**Result**
ATCC 27853 ***P. aeruginosa***		2µg/mL	S*
ATCC 25922 ***E. coli***		2µg/mL	S*
PAO1	Ancestral strain	2µg/mL	S
PAO1 A	*C. albicans*	4µg/mL	R
PAO1 B	*S. aureus*	4µg/mL	R
PAO1 C	*S. hominis*	2µg/mL	S
PAO1 D	*S. epidermidis*	2µg/mL	S
PAO1 E	*R. dentocariosa*	2µg/mL	S
PAO1 F	*R. mucilaginosa*	2µg/mL	S
PAO1 AE	*C. albicans* *R. dentocariosa*	2µg/mL	S
PAO1 BC	*S. aureus* *S. hominis*	4µg/mL	R
PAO1 DF	*S. epidermidis* *R. mucilaginosa*	2µg/mL	S
PAO1 BCD	*S. aureus* *S. hominis* *S. epidermidis*	2µg/mL	S
PAO1 AFE	*C. albicans* *R. mucilaginosa* *R. dentocariosa*	2µg/mL	S
PAO1 AD	*C. albicans* *S. epidermidis*	8µg/mL	R
PAO1 BF	*S. aureus* *R. mucilaginosa*	4µg/mL	R
PAO1 CE	*S. hominis* *R. dentocariosa*	2µg/mL	S
PAO1 ABC	*C. albicans* *S. aureus* *S. hominis*	8µg/mL	R
PAO1 DEF	*S. epidermidis* *R. dentocariosa* *R. mucilaginosa*	2µg/mL	S
PAO1 A-F	*C. albicans* *S. aureus* *S. hominis* *S. epidermidis* *R. dentocariosa* *R. mucilaginosa*	2µg/mL	S
PAO1 Evolved		2µg/mL	S

Table 6: Antibiotic susceptibility of evolved populations of *P. aeruginosa* (PAO1). Kirby-Bauer disc diffusion assays were used test whether populations of PAO1 (S1 and S2) isolated from various communities after the 10-day experiment, had altered antibiotic susceptibility profiles. Diameter of zone of inhibition (mm) were interpreted based on EUCAST guidelines, except for gentamicin which there is insufficient evidence for. Values are the average of three independent biological replicates. Green represents susceptibility and yellow represents intermediate resistance, based on EUCAST guidelines and diameter ranges. * Indicates zones of inhibition that contained heteroresistant colonies.

(A) S1 Populations	**Diameter of zone of inhibition (mm)**					
	GEN	**TOB**	**CAZ**	**CIP**	**MEM**	**TZP**
PAO1A	25	25	24	30	22	23
PAO1B	24	23	24	26	24	22
PAO1C	25	24	25	29	25	23
PAO1D	24	24	25	31	25	23
PAO1E	25	24	24	29	26	24
PAO1F	24	24	24	30	27	22
PAO1AE	25	24	23	29	27	23
PAO1BC	24	24	23	29	16*	23
PAO1DF	24	24	24	27	25	23
PAO1BCD	24	25	23	27	26	22
PAO1AFE	24	24	23	29	18*	23
PAO1AD	24	24	22	29	26*	23
PAO1BF	25	24	23	29	25*	22
PAO1CE	25	24	23	28	26	23
PAO1ABC	25	24	25	29	27*	24
PAO1DEF	25	23	24	29	27	24
PAO1 A-F	24	24	23	29	26	24
PAO1Evolved	24	24	24	30	26	23
ATCC	24	23	24	30	28	24

(B) S2 Populations	**Diameter of zone of inhibition (mm)**					
	GEN	**TOB**	**CAZ**	**CIP**	**MEM**	**TZP**
PAO1A	25	24	24	29	26	24
PAO1B	24	24	25	31	26	24
PAO1C	24	23	25	31	26	24
PAO1D	23	25	24	30	27	24
PAO1E	24	24	25	29	27	23
PAO1F	25	25	24	31	27	24
PAO1AE	25	25	24	30	28	23
PAO1BC	25	24	24	30	26	24
PAO1DF	23	23	24	30	26	23
PAO1BCD	24	23	24	30	25	23
PAO1AFE	24	23	25	28	24	23
PAO1AD	24	23	24	30	26	23
PAO1BF	23	24	24	29	28	24
PAO1CE	24	23	25	30	27	23
PAO1ABC	24	24	25	29	25	24
PAO1DEF	24	23	24	30	26	24
PAO1A-F	24	23	24	30	26	24
PAO1Evolved	24	23	24	28	27	22
ATCC	24	23	24	30	28	24

A

	MEM	
	Populations	**Clones**
PAO1AD	26	15
PAO1BC	16	15
PAO1AFE	18	16
PAO1BF	25	13
PAO1ABC	27	13

B

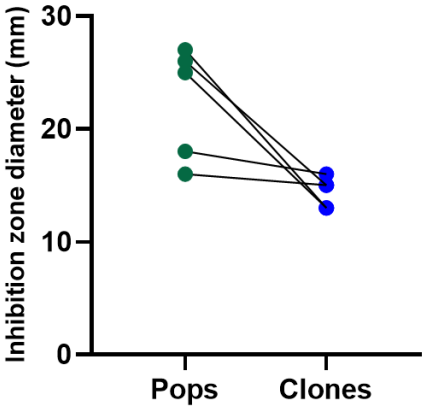

C

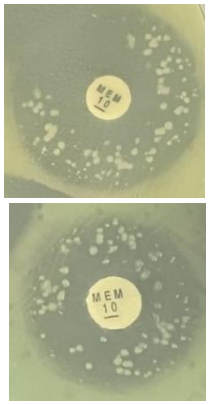

Fig. 13. Observation of heteroresistant clones arising from certain populations of PAO1 **(C)**. The values marked with an * from the S1 populations in **Table 6 (A)** were regrown and the Kirby-Bauer test using meropenem discs was performed again. A decrease in diameter size was seen from the heteroresistant colonies when compared to their respective populations **(B)**, with two populations BF and ABC, going from susceptible to resistant based on their sub-population **(A)**.

3.3.2.4 Colistin and Meropenem resistance may be linked to biofilms containing key species.

Biofilm assays were performed to assess if community context played a role in biofilm production and if key species produced more biofilm with *P. aeruginosa*. The partition communities were grown to allow biofilm formation before quantification via the crystal-violet staining method. Interestingly, *P.aeruginosa* produced more biofilm when grown with *C. albicans* (R1C1), and *S. aureus* (R1C2) (**Fig. 14).** Two- and three-species communities containing *S. aureus* and/or *C. albicans* also exhibited increased biofilm, indicating that these species are key to promoting *P. aeruginosa* biofilm, when compared to *P. aeruginosa* in a single-species biofilm. These results align with the colistin-resistance communities and the communities that had meropenem heteroresistance, with *S. aureus* and *C. albicans* being the common key species.

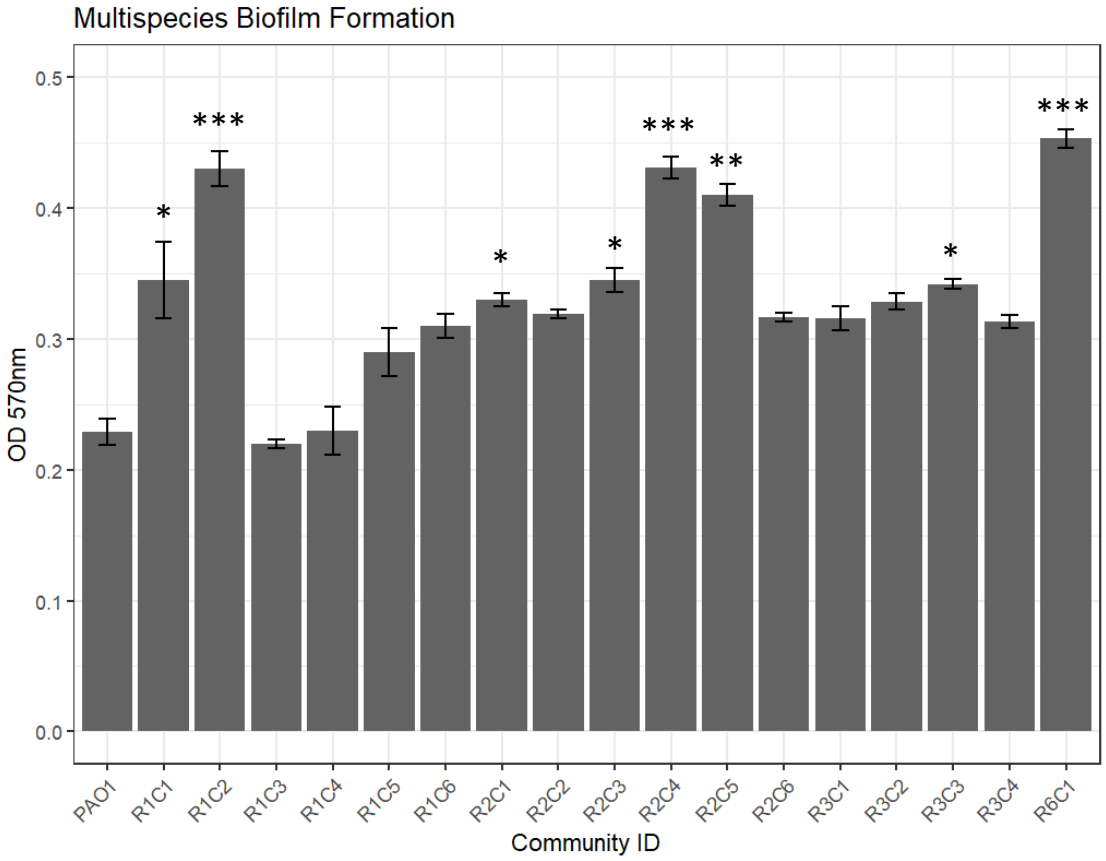

Fig. 14. *P. aeruginosa* in multispecies biofilms. The partition communities were set up as described in 3.2. They were allowed to grow for 24 hours before biofilm formation was assessed *via* the crystal violet staining method and absorbance (OD) was measured at 570nm. Values are the mean of three biological replicates ±SD. Kruskal Wallis, with Dunn post hoc tests were used to test for statistical significance between means of the groups when compared to PAO1 alone. **Note:** in this case, "PAO1" refers to the unevolved PAO1 ancestor, as these are not evolved populations, just a recreation of the short-term partition set up. Comparisons are denoted on the graph with asterisks representing significance (*p <0.05, **p <0.01, ***p<0.001).

3.3.2.5 *P. aeruginosa* morphology is influences by community context

Growth with *R. mucilaginosa* or *R. mucilaginosa*-containing communities results in two distinct *P. aeruginosa* phenotypes.

When PAO1 was plated onto C-N isolation agar, distinct colony morphotypes were seen depending on which community PAO1 was isolated from. We consistently observed that when PAO1 was isolated from a community containing *R. mucilaginosa*, two distinct colony phenotypes were observed **(Fig. 15B)**. These were visible at dilutions of 10^{-7} and 10^{-8} (**Fig. 15A**). A larger more irregular-edged colony type was seen (**Fig. 15C**) that was highly fluorescent suggesting pyoverdine and/or pyocyanin production. The second morphotype (**Fig. 15D**) had smaller round colonies and appeared to be more mucoid. This aligns with studies suggesting the co-existence of high virulent subtypes alongside low

secreting avirulent subtypes [12]. This change in *P. aeruginosa* colony morphology that is seen even after it is isolated suggests that growing in the presence of *R. mucilaginosa* drives phenotypic diversity in this pathogen, and that it is retained when the species is removed. *R. mucilaginosa* was found to be positively affecting pyocyanin production based on the linear model coefficients (**Fig. 8 A)** in the case of the S1 population set. The community ID that showed the most consistent emergence of these two morphotypes was R3C2 (comprising of species A, F, E). In the S1 population set, R3C2 had low pyocyanin production with no significant increase or decrease (**Fig. 7 A)**, however for S2 (**Fig. 7 B)**, R3C2 displays a significant increase in pyocyanin production**.** This once again highlights the variation in adaptation and emergence of different phenotypes in terms of virulence factor production. Pyocyanin production was tested for these subtypes, the suspected high producer fluorescent type (termed AFE.1), and the more mucoid type (AFE.2). This was only carried out once independently so statistical test could not be performed, but we can clearly see the stark difference in pyocyanin production of AFE.1 when compared to AFE.2, and the ancestral, evolved in isolation, and mutant strains (**Fig. 15 E).**

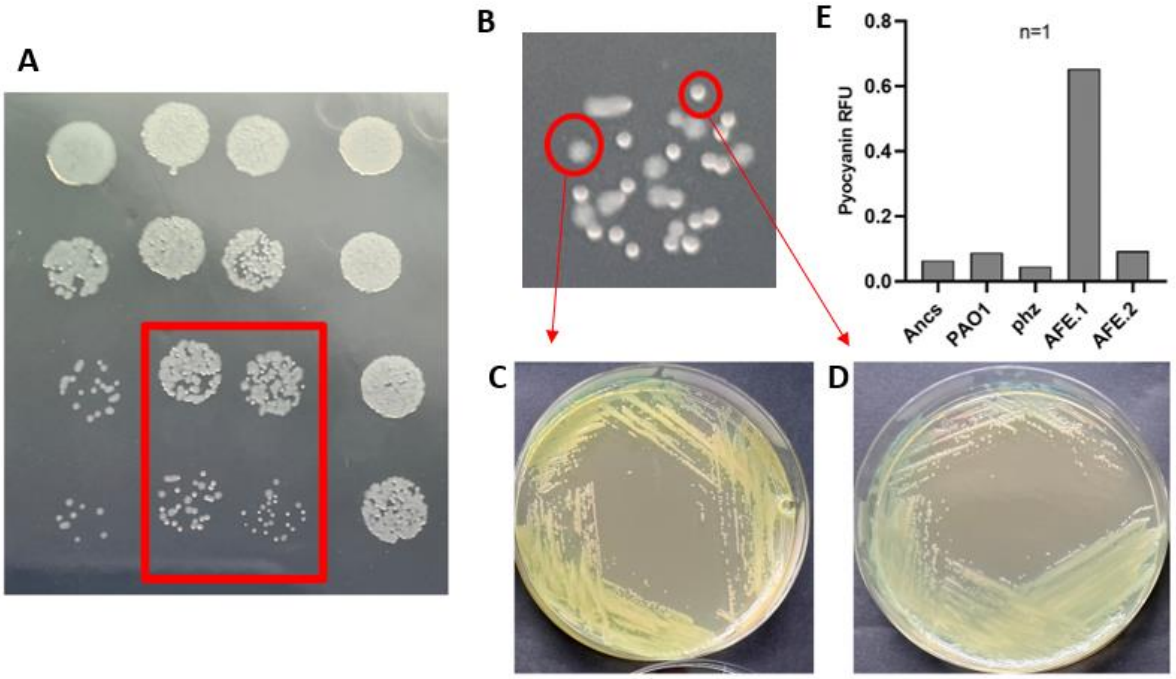

Fig. 15. Colony morphology of *P. aeruginosa* PAO1 grown on CN isolation agar **(A, B)**. Two distinct morphotypes were seen **(B)**, fluorescent, irregular-edged colony type **(C)**, and a smaller round mucoid colony type **(D)**. Termed AFE.1 **(C)** and AFE.2 **(D)**, a pyocyanin assay was conducted **(see methods xx)** to see if the two morphotypes differed in pyocyanin producing abilities and AFE.1, as suspected, had increased pyocyanin production when compared to the ancestor, PAO1 evolved alone and to its population neighbour AFE.2. As there is only an n=1, statistical analysis could not be performed but further replicates would confirm this initial observation.

3.4 Growth in Artificial Sputum

The complex nature of the CF lung environment is difficult to capture with lab experiments but is essential to understand how the oxygen and nutrient profiles, as well as mucin increase, can shape replicative niches and allow for pathogen adaptation. Artificial sputum media (ASM) was made using the protocol by Kirchner *et. al* [75]**.** Due to the length of this study, the partition could not be replicated in full in ASM, but since the media partition experiments revealed one-species communities (PAO1 and one other background species) were sufficient to predict dynamics of more diverse communities, these communities were tested in ASM. The CF isolate LESB58 was also included as it would be expected to do better in a more CF-like environment compared to the "CF-naïve" PAO1 strain.

All PAO1 community strains **(Fig. 16A)** had significantly decreased final densities when compared to PAO1 grown alone (Wilcoxon rank-sum test; R1C1=p<0.05, R1C3=p<0.05, R1C4=p<0.05, R1C5=p<0.05, R1C6=p<0.01), except PAO1 R1C2 (*S. aureus*). LESB58 strains **(Fig. 16B)** isolated from R1C2 (*S. aureus*), R1C4 (*S. epidermidis*), and R1C6 (*R. mucilaginosa*) had significantly higher final densities compared to LESB58 grown alone, (Wilcoxon rank-sum test; R1C2=p<0.05, R1C4=p<0.05, R1C6=p<0.05). LESB58 isolated from *C. albicans* (R1C1) was found to have a significantly decreased final density compared to the control, (Wilcoxon rank-sum test; R1C1=p<0.01).

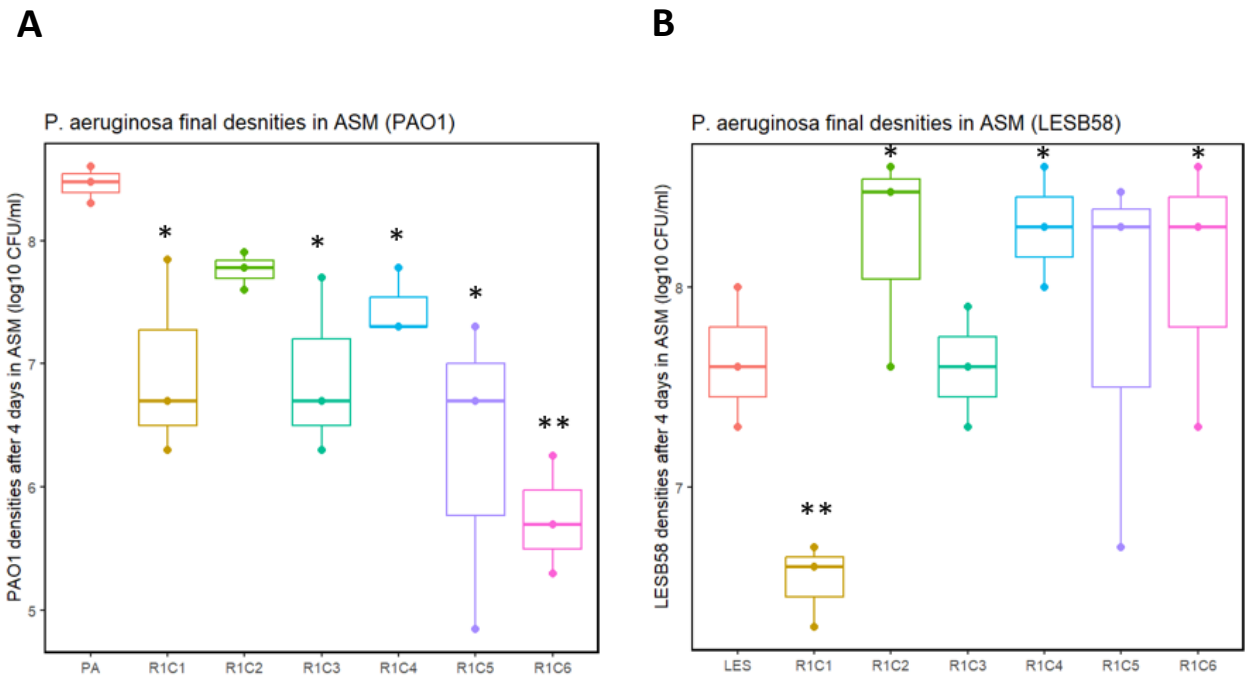

Fig. 16. Final densities of *P. aeruginosa*, PAO1 **(A)** and LESB58 **(B)** in artificial sputum medium (ASM) after 4 days of growth. PAO1 and LESB58 were each grown with each of the six background species (R=1) in ASM. All PAO1 community strains **(A)** had significantly decreased final densities when compared to PAO1 grown alone, except PAO1 R1C2 (*S. aureus*). LESB58 strains **(B)** isolated

from R1C2 (*S. aureus*), R1C4 (*S. epidermidis*), and R1C6 (*R. mucilaginosa*) had significantly higher densities than LESB58 while R1C1 (*C. albicans*) had significantly decreased final density compared to LESB58 alone. The experiment was repeated three times independently, and n=3 biological replicates are shown. Asterisks represent significance when comparing PAO1 or LESB58 isolated from communities to their respective controls grown without any species. Wilcoxon rank-sum tests, (*p <0.05, **p <0.01, ***p<0.001). PA=PAO1, LES=LESB58, "R1C1" in **(A)** refers to PAO1 isolated from community R1C1; (*C. albicans* and in **(B)** refers to LESB58 isolated from community R1C1; (*C. albicans*).

4. DISCUSSION

Addressing the complexity of microbial communities has become a key element in understanding disease in the last decade. This study investigated the effects of microbial background communities on the growth and virulence of the predominant CF pathogen *P. aeruginosa*, more pertinently, the effects of species richness *versus* species composition. With the widespread acknowledgement of CF as a polymicrobial disease with unique within-patient diversity [5], it has become essential to study pathogens not in isolation, but as part of communities interacting on various levels. This ecological understanding of microbial community context may help bridge the gap between clinical studies and predictions of disease variation and patient prognosis.

To tease apart the effects of species richness *versus* composition, a random partition design [61] was used. The results of this experiment allowed us to establish the model, which had originally only been applied to soil organisms [63-66], for a more clinical set of microbes and use it to identify the relative importance of bacterial richness and composition in driving *P. aeruginosa* growth and clinically-relevant phenotypes. We found that species composition (absences and presence of key species) had a more pronounced effect on final densities of *P. aeruginosa* as opposed to richness (the number of species present) in both the short-term and extended partition experiments. We know that ecological interactions such as interbacterial competition can shape community structure and pathogenesis, but there may be other factors at play. Priority effects have recently gained renewed interest to study community assembly [78], where the impact a species exerts on other species depends on the species arrival order into the community [79]. In a bacterial community context for human disease, it can be described as the impact of early colonisers on a later coloniser within a community [80, 81]. This framework was applied to the random partition model with staggered inoculation, where the background community was given "priority" and time to stabilise before the pathogen inoculation, crudely mimicking *P. aeruginosa* invasion and colonisation in the lungs.

We found that in the short-term partition experiment (**Fig. 3, Fig. 4)**, that species composition had a significant effect on *P. aeruginosa* final densities. Using the linear coefficients, the model picked out *C. albicans* and *R. mucilaginosa* to be positively affecting *P. aeruginosa* growth, while *S. hominis*, and to a lesser extent, *S. epidermidis* were found to negatively affect growth. Many studies have shown fungal-bacterial interactions in the context of CF, specifically looking at *C. albicans* and *P. aeruginosa* [58, 77, 82]. It has been shown that coexistence of *C. albicans* with *P. aeruginosa* can enhance biofilm via alginate-related extracellular matrix proteins as *C. albicans* increases ECM production in *P. aeruginosa* [83]. This corroborates studies on multispecies biofilms and may explain the higher densities of *P. aeruginosa* in my experiment in the presence of *C. albicans* [80, 83, 84]. The

morphological state of *C. albicans i.e.* hyphal or yeast form, was not examined during the experiment and may be of interest.

The supernatant assay results, while preliminary, showed contrasting results to the trends seen in the partition experiment, particularly in the case of *C. albicans*. While in the partitions, we found *C. albicans* to be promoting *P. aeruginosa* final densities, we see its supernatant inhibiting *P. aeruginosa* growth when compared to the control (**Fig. 2**). This may suggest that *C. albicans* secretes some inhibitory molecule which may be found in the supernatant but raises the question as to why this inhibitory effect is reversed when the species are grown in co-culture as in the partition. Further replicates of the supernatant assay may identify this contradicting result. Furthermore the supernatant assay was performed under shaking conditions, while the partitions were static and this may have played a role in the spatial structure and distribution of secreted molecules due to the biofilm nature of the cultures [85].

R. mucilaginosa was consistently found to be significantly increasing *P. aeruginosa* final densities, and communities that contained this species followed this promoting effect. While there is limiting research into *P. aeruginosa* and *R. mucilaginosa* interactions in lung disease, some studies have elucidated the effect of *R. mucilaginosa* metabolites in promoting *P. aeruginosa* growth and a similar phenomenon may be occurring here. A study investigating the CF lung microbiome found that *R. mucilaginosa* boosts *P. aeruginosa* growth *via* metabolite cross-talk and cross-feeding mechanisms [86, 87]. The role of *Rothia* spp. in the context of CF and its interactions with pathogens is not known. However, due to its putative metabolic versatility, for example, fermenting complex carbohydrates into metabolites such as short-chain fatty acids or amino acids, it has been suggested that ecologically it could serve as a supplier of substrates for more-specialised community members such as *P. aeruginosa*, particularly sub-populations that cannot degrade mucin [52, 86]. Hence, the communities containing *R. mucilaginosa* and/or *C. albicans* may be expected to facilitate an increased chance of successful *P. aeruginosa* establishment.

While the specific contributions of *S. hominis* to CF community context requires further elucidation, it is evident that its potential role in inhibition of *P. aeruginosa* growth highlights the importance of focusing on microbial ecology and community dynamics in order to develop targeted therapeutic approaches that consider the complex polymicrobial nature of CF infections. It also shows how overlooked microbiomes such as opportunistic members of the skin and mucosal communities may be a potential area of focus when investigating species interactions with focal CF pathogens.

Selective pressures during chronic infection (imitated crudely by the extended partition experiment), can drive both microbial competition and cooperation [88]. Extending the short-term partition allowed us to see if the effects seen short-term were sustained over a longer period of time as *P. aeruginosa*

adapted to the communities as this is what is seen in CF infection [11]. While there was no statistically significant effect of species richness or composition on final densities in the extended partition, we did see a similar trend of composition, and more importantly, key individual species (**Fig.6**) playing a modulatory role, as we observed in the short-term experiment.

It has been shown that species interactions may evolve to be less negative over time, particularly in more diverse communities [63]. Species may be able to "block" *P. aeruginosa* initially (short-term), but overall cannot compete long-term (extended) or sustain this blocking [22]. The short-term partition effects not being evident in the longer extended partition highlights the importance of long-term evolution experiments, comprising of diverse microbial communities, to understand the ever-changing evolutionary landscape in chronic infections such as CF where dynamic pathogens like *P. aeruginosa* adapt and undergo many phenotypic and genotypic changes. The long-term loss of competition may be coupled with the naïve *P. aeruginosa* (PAO1) adapting to the background communities *via* various pathoadaptive phenotypes and alterations in virulence factor expression [11].

The consistent insignificance of richness level 6, while showing that more diverse communities aren't necessarily more efficient at preventing pathogen colonisation and growth resistance, may also just be a result of overcrowding of species and resource competition *in vitro.* This would need to be repeated in ASM or *in vivo* with a more detailed look on the species interactions, to pinpoint what exactly is causing this. Furthermore, it was not feasible in this experimental timeframe/set up, nor was it part of the scope of this project to track the densities and relative abundances of the background community members. However, we accept that this is a crucial limitation and must be focused on in future experiments. In higher richness levels, as time progresses, it is likely that *P. aeruginosa* adapted quickly and, in some communities, employed virulence factors to outcompete and kill other species. This would automatically result in lower abundances of other species and higher ones of *P. aeruginosa*.

Due to the complex nature of each polymicrobial assemblage and the numerous combinations, it is difficult to distinguish between indirect and direct effects of the species on *P. aeruginosa.* For example, in communities with staphylococci, the species may not be directly affecting *P. aeruginosa* but it has been shown that Esp from *S. epidermidis* can degrade proteins associated with *S. aureus* biofilm formation [89]. This competitive behaviour may in turn, indirectly benefit *P. aeruginosa* growth. Background community interactions can provide replicative and nutritional "space" and dampen the effects of species that would otherwise inhibit *P. aeruginosa.*

It is important to note that the partition experiments were carried out static and not shaking created a semi-structured environment which would affect dispersal and diffusion of metabolites and alter metabolic dynamics. While the structure was disturbed daily during the transfers in the extended partition, overall, we can assume there was a structured environment and we could expect to see

different results if these experiments were carried out shaking, as were most of the phenotypic analyses. It has been shown that structured and static environments can alter the relative fitness and competitive outcomes of *P.* aeruginosa when grown in co-culture with *S. aureus* [90]. The ASM provided a very structured environment mimicking the heavy mucus composition in the CF airways. The complexity of bacterial-bacterial interactions in a spatially structured environment such as ASM, with the added variable of oxygen levels, provides an insight into the effects of environment on pathogenic trajectories in chronic infection.

To test the effects of community context on secreted virulence products in the panel of evolved populations, the phenazine pyocyanin was measured due to its putative role as potent virulence factor in *P. aeruginosa* and also its ability to act as a quorum sensing molecule often involved in biofilm stability [91, 92]. The inhibitory effects of *C. albicans*-containing communities on pyocyanin production corroborates literature on the interplay between fungal farnesol and phenazine interactions *via* inhibition of QS [57, 92]. Many studies have shown that *C. albicans* produces ethanol and farnesol in co-culture with *P. aeruginosa* and can affect phenazine production via stimulation of quorum sensing signalling [55-58], and this may be occurring in our coculture experiments.

The primary siderophore pyoverdine was also measured. This iron-chelator is essential for *P. aeruginosa* to thrive in environments of low iron availability [12]. In the CF lung, iron levels are elevated [93] and so we expect adapted CF isolates of *P. aeruginosa* to undergo potential loss of function mutations for siderophore biosynthesis genes as there is no need to employ such a metabolically costly nutrient uptake mechanism. It is possible that the simple adaptation to the lab media and environment also drives loss of function mutations [94].

A significant loss of pyoverdine was seen in many of the S2 populations, compared to the ancestor, but this trend was not visible in the S1 populations. While S1 and S2 populations are replicates and began from the same ancestor, it is likely that they followed different trajectories of adaptations during the 10-day experiment, displaying phenotypic alterations, and possibly acquiring *de novo* point mutations [20]. A similar phenomenon can be seen in the most well-known and longest running long-term evolution experiment by Richard Lenski [95] and colleagues, where initial identical populations began to display altered phenotypes and metabolic capabilities. The most notable being the Ara-3 population which was found to contain clones that were able to grow aerobically on citrate [96]. This highlights the ever-changing dynamics of adaptation in microbial populations.

The polymicrobial nature of the CF airways is likely to have a significant impact on the clinical response to antimicrobial therapy and this was evident via the antimicrobial susceptibility testing of the evolved populations from the extended partition. Interesting trends were observed that both corroborated with and contradicted previous studies. Colistin susceptibility was tested via MICs using the microbroth

dilution method. For the six communities where *C. albicans* was present, three contained colistin resistant *P. aeruginosa*. This finding can be compared to a recent study that showed that *C. albicans* enhanced meropenem tolerance of *P. aeruginosa* [97]. This also recapitulates the putative interkingdom fungal-bacterial interactions between these species, and ultimately highlights how these interactions can affect antibiotic responses and clinical outcomes [98]. Interestingly, when *R. dentocariosa* was present alongside *C. albicans* (i.e. the remaining three communities), no colistin resistance was observed in *P. aeruginosa*. This suggests that *R. dentocariosa* could ameliorate the evolution of colistin resistance in *P. aeruginosa*, although this would need to be verified experimentally.

We found that evolved PAO1 populations isolated from communities containing *S. aureus* were resistant to colistin. A previous study [60] found that LPS is truncated in *P. aeruginosa* in response to *S. aureus*, which may affect overall envelope charge and impact of colistin resistance. The correlation between biofilm formation and decreased antibiotic permeability has been studied extensively in many nosocomial pathogens such as *Klebsiella pneumoniae* [99], particularly looking at carbapenem-resistance. While there are studies showing *P. aeruginosa* forms robust biofilms with *C. albicans* and *S. aureus*, there is little work linking these multispecies biofilms and their ecology to colistin and meropenem resistance [41, 100]. The biofilm results presented align with the colistin-resistance communities and the communities that had meropenem heteroresistance, with *S. aureus* and *C. albicans* being the common key species. These data suggest that these key species promote biofilm formation with *P. aeruginosa*, which in turn may indirectly lead to colistin and meropenem resistance.

Dual-species biofilms between *P. aeruginosa* and *C. albicans*, and *S. aureus* have been extensively described in the literature. Interactions within the biofilm can have implications for disease progression and antibiotic treatment. Our linked antibiotic resistance and biofilm data suggest that a synergistic resistance interaction of may be occurring with *P. aeruginosa* and *S. aureus* co-existing in this biofilm mode [101]. In this microenvironment, stress induced by one species may trigger a resistance mechanism in the other which would overall enhance the resistance profile coupled with the added biofilm matrix [102]. It has been shown that multispecies biofilm with *C. albicans* increases the resistance of *P. aeruginosa* to meropenem within their mixed-species biofilm [97]. *C. albicans* may also promote *P. aeruginosa* biofilm formation by modulating its las/rhl QS system [103] which in turn can increase antibiotic resistance. Our observations with these multispecies biofilms and antibiotic resistance profiles for colistin and meropenem corroborate existing studies, and once again highlight the importance of polymicrobial interactions in infection and how the inevitable biofilm formation between these species can greatly worsen clinical outcomes in CF [13, 44].

The co-existence of highly virulent pathotypes of *P. aeruginosa* with more avirulent subtypes can be seen in the CF airways [12]. In this study, growth with *R. mucilaginosa*-containing communities induced the emergence of two distinct colony phenotypes of *P. aeruginosa*, with one displaying

increased pyocyanin production (n=1) and therefore, likely increased virulence. The effects of certain species promoting sub-populations of varying virulence in *P. aeruginosa* is of clinical significance when taken into the account the stark within-patient diversity of CF isolates. While studies have investigated abiotic drivers, such as antibiotic use, of these adaptations in depth, it may be of relevance to hone in on biotic factors, that is, the microbial community context. Understanding keystone species effects may shed light on what existing microbiome compositions are more efficient in withstanding *P. aeruginosa* colonisation and which species may exacerbate the virulence of this pathogen.

The findings from this study can be applied broadly to the idea that while species richness/diversity may play an important role in microbial communities affecting pathogen virulence, these virulence trajectories and clinically pertinent phenotypes seem to be more affected by species composition. The presence of certain key species (such as those identified in this study) can overpower the effects of richness and induce promoting or inhibiting effects on virulence factor production of *P. aeruginosa*.

OUTLOOK AND FUTURE PROSPECTS

There is compelling evidence that multispecies interactions can modify the virulence capacity of *P. aeruginosa* short-term, as we have shown in this study, but also influence the pathogen's evolutionary course long-term. In recent years, our understanding of *P. aeruginosa' s* response to other species has greatly improved, but it is still unknown how these interactions affect virulence and clinically relevant phenotypes in a complex multispecies community. This study aimed to address this aspect using the random partition model and synthetic microbial communities.

Understanding the extent to which virulence factors are influenced by members of the lung microbiome is an avenue for novel therapeutics in chronic lung infections. Building onto the community context framework established in this study could allow the development of "colonisation resistant" microbial communities that can withstand initial colonisation by pathogens, or the creation of communities comprising of commensals that can ameliorate virulence or alter pathoadaptive trajectories.

While the scope and length of this project did not allow further investigations into many novel findings, it provides a framework from which to carry on future work, highlighting key interactions and species combinations that should be studied in order to understand the effects of community context on *P. aeruginosa*. This work also provides proof-of-concept via the application of the Bell model to study microbial communities relevant to human disease, which had not previously been done. This study highlights the benefits of studying human infection through an ecological lens and approaching CF as a polymicrobial disease. It also shows that short-term effects of microbial species dynamics don't

always translate long-term, and there is a need for experimental evolution when trying to understand the evolutionary changes pathogens and commensals undergo during sustained chronic infection.

It would be interesting to follow this work on, focusing on attempting to replicate the extended partition experiments in ASM and honing in on particular interactions such as the bacterial-fungal network of *P. aeruginosa* and *C. albicans*, the seemingly antagonistic relationship between *P. aeruginosa* and *S. hominis,* and to further elucidate metabolic factors of oral commensals such as *R. mucilaginosa* with respect to their role in potentially driving *P. aeruginosa* growth. Sequencing the evolved PAO1 populations from the extended partition experiment may reveal some mutations, despite this experiment not being the classical length to be termed "long-term evolution".

Ecological concepts such as the "keystone species" that maintain homeostasis in the microbial community of the lungs and respiratory tract remain poorly understood. It remains unclear the state of dysbiosis that precedes *P. aeruginosa* colonisation. An approach to investigate this may involve longitudinal sampling of the airways [23, 104] prior to the establishment of a dominant pathogen such as *P. aeruginosa*, particularly if it is displacing the pre-existing pathogen *S. aureus.*

This work can be seen as a proof-of-concept study and preliminary research in the establishment of a framework that allows us to predict how various ecological interactions between pathogens and commensals, or just between microbial species, affect virulence of focal pathogens in polymicrobial infections, such as *P. aeruginosa* in CF. The applications for this partition model approach are broad and can be applied to model polymicrobial disease in various sites of infection. From the findings of this study, we once again highlight how important it is to study the ecological interactions between pathogens and commensals in microbial communities, as they may shed light onto unresolved aspects of polymicrobial infections in human disease.

5. REFERENCES

1. Jurado-Martín, I., M. Sainz-Mejías, and S. McClean, *Pseudomonas aeruginosa: An Audacious Pathogen with an Adaptable Arsenal of Virulence Factors.* International Journal of Molecular Sciences, 2021. **22**(6): p. 3128.
2. Miller, W.R. and C.A. Arias, *ESKAPE pathogens: antimicrobial resistance, epidemiology, clinical impact and therapeutics.* Nature Reviews Microbiology, 2024. **22**(10): p. 598-616.
3. Elfadadny, A., et al., *Antimicrobial resistance of Pseudomonas aeruginosa: navigating clinical impacts, current resistance trends, and innovations in breaking therapies.* Frontiers in Microbiology, 2024. **15**.
4. Santajit, S. and N. Indrawattana, *Mechanisms of Antimicrobial Resistance in ESKAPE Pathogens.* Biomed Res Int, 2016. **2016**: p. 2475067.
5. Reece, E., P.H.d.A. Bettio, and J. Renwick, *Polymicrobial Interactions in the Cystic Fibrosis Airway Microbiome Impact the Antimicrobial Susceptibility of Pseudomonas aeruginosa.* Antibiotics, 2021. **10**(7): p. 827.
6. LiPuma, J.J., *The Changing Microbial Epidemiology in Cystic Fibrosis.* Clinical Microbiology Reviews, 2010. **23**(2): p. 299-323.
7. Sanya, D.R.A., et al., *Recent advances in therapeutic targets identification and development of treatment strategies towards Pseudomonas aeruginosa infections.* BMC Microbiology, 2023. **23**(1): p. 86.
8. Cuthbertson, L., et al., *Lung function and microbiota diversity in cystic fibrosis.* Microbiome, 2020. **8**(1): p. 45.
9. Vandeplassche, E., et al., *Antibiotic susceptibility of cystic fibrosis lung microbiome members in a multispecies biofilm.* Biofilm, 2020. **2**: p. 100031.
10. Bartell, J.A., et al., *Evolutionary highways to persistent bacterial infection.* Nat Commun, 2019. **10**(1): p. 629.
11. Winstanley, C., S. O'Brien, and M.A. Brockhurst, *Pseudomonas aeruginosa Evolutionary Adaptation and Diversification in Cystic Fibrosis Chronic Lung Infections.* Trends in Microbiology, 2016. **24**(5): p. 327-337.
12. O'Brien, S., et al., *High virulence sub-populations in Pseudomonas aeruginosa long-term cystic fibrosis airway infections.* BMC Microbiology, 2017. **17**(1): p. 30.
13. O'Brien, S. and J.L. Fothergill, *The role of multispecies social interactions in shaping Pseudomonas aeruginosa pathogenicity in the cystic fibrosis lung.* FEMS Microbiology Letters, 2017. **364**(15).

14. Cox, M.J., et al., *Airway Microbiota and Pathogen Abundance in Age-Stratified Cystic Fibrosis Patients.* PLOS ONE, 2010. **5**(6): p. e11044.
15. Nelson, A., et al., *Polymicrobial challenges to Koch's postulates: Ecological lessons from the bacterial vaginosis and cystic fibrosis microbiomes.* Innate Immunity, 2012. **18**(5): p. 774-783.
16. Harrison, F., *Microbial ecology of the cystic fibrosis lung.* Microbiology, 2007. **153**(4): p. 917-923.
17. Harrison, F., et al., *Interspecific competition and siderophore-mediated cooperation in Pseudomonas aeruginosa.* ISME J, 2008. **2**(1): p. 49-55.
18. Leinweber, A., M. Weigert, and R. Kummerli, *The bacterium Pseudomonas aeruginosa senses and gradually responds to interspecific competition for iron.* Evolution, 2018. **72**(7): p. 1515-28.
19. Gao, B., et al., *Tracking Polymicrobial Metabolism in Cystic Fibrosis Airways: Pseudomonas aeruginosa Metabolism and Physiology Are Influenced by Rothia mucilaginosa-Derived Metabolites.* mSphere, 2018. **3**(2).
20. Vandeplassche, E., et al., *In vitro evolution of Pseudomonas aeruginosa AA2 biofilms in the presence of cystic fibrosis lung microbiome members.* Scientific Reports, 2019. **9**(1): p. 12859.
21. Carmody, L.A., et al., *Changes in Cystic Fibrosis Airway Microbiota at Pulmonary Exacerbation.* Annals of the American Thoracic Society, 2013. **10**(3): p. 179-187.
22. Spragge, F., et al., *Microbiome diversity protects against pathogens by nutrient blocking.* Science, 2023. **382**(6676): p. eadj3502.
23. Yagi, K., et al., *The Lung Microbiome during Health and Disease.* International Journal of Molecular Sciences, 2021. **22**(19): p. 10872.
24. Li, R., J. Li, and X. Zhou, *Lung microbiome: new insights into the pathogenesis of respiratory diseases.* Signal Transduction and Targeted Therapy, 2024. **9**(1): p. 19.
25. Fothergill, J.L., et al., *Pseudomonas aeruginosa adaptation in the nasopharyngeal reservoir leads to migration and persistence in the lungs.* Nature Communications, 2014. **5**(1): p. 4780.
26. Wang, G. and W.M. Nauseef, *Neutrophil dysfunction in the pathogenesis of cystic fibrosis.* Blood, 2022. **139**(17): p. 2622-2631.
27. Arai, H., *Regulation and Function of Versatile Aerobic and Anaerobic Respiratory Metabolism in Pseudomonas aeruginosa.* Frontiers in Microbiology, 2011. **2**.
28. Whiley, R.A., et al., *Environment and Colonisation Sequence Are Key Parameters Driving Cooperation and Competition between Pseudomonas aeruginosa Cystic Fibrosis Strains and Oral Commensal Streptococci.* PLOS ONE, 2015. **10**(2): p. e0115513.
29. Mammen, M.J., F.A. Scannapieco, and S. Sethi, *Oral-lung microbiome interactions in lung diseases.* Periodontol 2000, 2020. **83**(1): p. 234-241.

30. Tian, S., T. Ding, and H. Li, *Oral microbiome in human health and diseases.* mLife, 2024. **3**(3): p. 367-383.
31. La Rosa, R., H.K. Johansen, and S. Molin, *Adapting to the Airways: Metabolic Requirements of Pseudomonas aeruginosa during the Infection of Cystic Fibrosis Patients.* Metabolites, 2019. **9**(10): p. 234.
32. Schiessl, K.T., et al., *Phenazine production promotes antibiotic tolerance and metabolic heterogeneity in Pseudomonas aeruginosa biofilms.* Nature Communications, 2019. **10**(1): p. 762.
33. Hesse, E. and S. O'Brien, *Ecological dependencies and the illusion of cooperation in microbial communities.* Microbiology, 2024. **170**(2).
34. Baty, J.J., et al., *A Commensal Streptococcus Dysregulates the Pseudomonas aeruginosa Nitrosative Stress Response.* Frontiers in Cellular and Infection Microbiology, 2022. **12**.
35. Sheldon, J.R. and D.E. Heinrichs, *Recent developments in understanding the iron acquisition strategies of gram positive pathogens.* FEMS Microbiol Rev, 2015. **39**(4): p. 592-630.
36. Page, M.G.P., *The Role of Iron and Siderophores in Infection, and the Development of Siderophore Antibiotics.* Clin Infect Dis, 2019. **69**(Suppl 7): p. S529-S537.
37. Holden, V.I. and M.A. Bachman, *Diverging roles of bacterial siderophores during infection.* Metallomics, 2015. **7**(6): p. 986-95.
38. Bottery, M.J., et al., *Co-occurring microflora and mucin drive Pseudomonas aeruginosa diversification and pathoadaptation.* ISME Communications, 2024. **4**(1).
39. Cramer, N., et al., *Competitive fitness of Pseudomonas aeruginosa isolates in human and murine precision-cut lung slices.* Front Cell Infect Microbiol, 2022. **12**: p. 992214.
40. O'Brien, S., M. Baumgartner, and A.R. Hall, *Species interactions drive the spread of ampicillin resistance in human-associated gut microbiota.* Evolution, Medicine, and Public Health, 2021. **9**(1): p. 256-266.
41. Bottery, M.J., et al., *Inter-species interactions alter antibiotic efficacy in bacterial communities.* The ISME Journal, 2022. **16**(3): p. 812-821.
42. Hammer, N.D. and E.P. Skaar, *Molecular mechanisms of Staphylococcus aureus iron acquisition.* Annu Rev Microbiol, 2011. **65**: p. 129-47.
43. Emerson, J., et al., *Pseudomonas aeruginosa and other predictors of mortality and morbidity in young children with cystic fibrosis.* Pediatr Pulmonol, 2002. **34**(2): p. 91-100.
44. Camus, L., et al., *How Bacterial Adaptation to Cystic Fibrosis Environment Shapes Interactions Between Pseudomonas aeruginosa and Staphylococcus aureus.* Front Microbiol, 2021. **12**: p. 617784.

45. Briaud, P., et al., *Coexistence with Pseudomonas aeruginosa alters Staphylococcus aureus transcriptome, antibiotic resistance and internalization into epithelial cells.* Scientific Reports, 2019. **9**(1): p. 16564.
46. Bernardy, E.E., V. Raghuram, and J.B. Goldberg, *Staphylococcus aureus and Pseudomonas aeruginosa Isolates from the Same Cystic Fibrosis Respiratory Sample Coexist in Coculture.* Microbiol Spectr, 2022. **10**(4): p. e0097622.
47. Pajon, C., et al., *Interactions between metabolism and growth can determine the co-existence of Staphylococcus aureus and Pseudomonas aeruginosa.* eLife, 2023. **12**: p. e83664.
48. Otto, M., *Staphylococcus epidermidis — the 'accidental' pathogen.* Nature Reviews Microbiology, 2009. **7**(8): p. 555-567.
49. Fernández-Fernández, R., et al., *Bacteriocin-Like Inhibitory Substances in Staphylococci of Different Origins and Species With Activity Against Relevant Pathogens.* Frontiers in Microbiology, 2022. **13**.
50. Kim, P.I., et al., *Characterization and structure identification of an antimicrobial peptide, hominicin, produced by Staphylococcus hominis MBBL 2–9.* Biochemical and Biophysical Research Communications, 2010. **399**(2): p. 133-138.
51. O'Sullivan, J.N., et al., *Human skin microbiota is a rich source of bacteriocin-producing staphylococci that kill human pathogens.* FEMS Microbiology Ecology, 2018. **95**(2).
52. Uranga, C.C., et al., *Commensal Oral Rothia mucilaginosa Produces Enterobactin, a Metal-Chelating Siderophore.* mSystems, 2020. **5**(2).
53. O'Brien, S. and J.L. Fothergill, *The role of multispecies social interactions in shaping Pseudomonas aeruginosa pathogenicity in the cystic fibrosis lung.* FEMS Microbiol Lett, 2017. **364**(15).
54. Tyrrell, J. and M. Callaghan, *Iron acquisition in the cystic fibrosis lung and potential for novel therapeutic strategies.* Microbiology (Reading), 2016. **162**(2): p. 191-205.
55. Décanis, N., et al., *Farnesol, a fungal quorum-sensing molecule triggers Candida albicans morphological changes by downregulating the expression of different secreted aspartyl proteinase genes.* Open Microbiol J, 2011. **5**: p. 119-26.
56. De Sordi, L. and F.A. Mühlschlegel, *Quorum sensing and fungal–bacterial interactions in Candida albicans: a communicative network regulating microbial coexistence and virulence.* FEMS Yeast Research, 2009. **9**(7): p. 990-999.
57. Doing, G., et al., *Conditional antagonism in co-cultures of Pseudomonas aeruginosa and Candida albicans: An intersection of ethanol and phosphate signaling distilled from dual-seq transcriptomics.* PLoS Genet, 2020. **16**(8): p. e1008783.

58. Cugini, C., D.K. Morales, and D.A. Hogan, *Candida albicans-produced farnesol stimulates Pseudomonas quinolone signal production in LasR-defective Pseudomonas aeruginosa strains.* Microbiology (Reading), 2010. **156**(Pt 10): p. 3096-3107.
59. Bansept, F., et al., *Modeling host-associating microbes under selection.* The ISME Journal, 2021. **15**(12): p. 3648-3656.
60. Tognon, M., et al., *Co-evolution with Staphylococcus aureus leads to lipopolysaccharide alterations in Pseudomonas aeruginosa.* Isme j, 2017. **11**(10): p. 2233-2243.
61. Bell, T., et al., *A Linear Model Method for Biodiversity–Ecosystem Functioning Experiments.* The American Naturalist, 2009. **174**(6): p. 836-849.
62. Evans, R., et al., *Defining the functional traits that drive bacterial decomposer community productivity.* The ISME Journal, 2017. **11**(7): p. 1680-1687.
63. Fiegna, F., et al., *Evolution of species interactions determines microbial community productivity in new environments.* The ISME Journal, 2015. **9**(5): p. 1235-1245.
64. Xiong, X., et al., *Keystone species determine the "selection mechanism" of multispecies biofilms for bacteria from soil aggregates.* Science of The Total Environment, 2021. **773**: p. 145069.
65. Wu, F., et al., *Modulation of microbial community dynamics by spatial partitioning.* Nat Chem Biol, 2022. **18**(4): p. 394-402.
66. Rivett, D.W., et al., *Resource-dependent attenuation of species interactions during bacterial succession.* The ISME Journal, 2016. **10**(9): p. 2259-2268.
67. Bestion, E., et al., *Phytoplankton biodiversity is more important for ecosystem functioning in highly variable thermal environments.* Proc Natl Acad Sci U S A, 2021. **118**(35).
68. Mowat, E., et al., *Pseudomonas aeruginosa population diversity and turnover in cystic fibrosis chronic infections.* Am J Respir Crit Care Med, 2011. **183**(12): p. 1674-9.
69. Choi, J.W., S.-H. Lee, and S.-G. Chung, *Relation of microbial biomass to counting units for Pseudomonas aeruginosa.* African journal of microbiology research, 2012. **6**: p. 4620-4622.
70. Buckling, A., et al., *The Beagle in a bottle.* Nature, 2009. **457**(7231): p. 824-829.
71. Dumas, Z., A. Ross-Gillespie, and R. Kümmerli, *Switching between apparently redundant iron-uptake mechanisms benefits bacteria in changeable environments.* Proc Biol Sci, 2013. **280**(1764): p. 20131055.
72. Burmølle, M., et al., *Enhanced Biofilm Formation and Increased Resistance to Antimicrobial Agents and Bacterial Invasion Are Caused by Synergistic Interactions in Multispecies Biofilms.* Applied and Environmental Microbiology, 2006. **72**(6): p. 3916-3923.
73. Yusuf, E., et al., *The accuracy of four commercial broth microdilution tests in the determination of the minimum inhibitory concentration of colistin.* Annals of Clinical Microbiology and Antimicrobials, 2020. **19**(1): p. 42.

74. Satlin, M.J., et al., *Clinical and Laboratory Standards Institute and European Committee on Antimicrobial Susceptibility Testing Position Statements on Polymyxin B and Colistin Clinical Breakpoints.* Clin Infect Dis, 2020. **71**(9): p. e523-e529.
75. Kirchner, S., et al., *Use of artificial sputum medium to test antibiotic efficacy against Pseudomonas aeruginosa in conditions more relevant to the cystic fibrosis lung.* J Vis Exp, 2012(64): p. e3857.
76. Zuur, A.F. and E.N. Ieno, *A protocol for conducting and presenting results of regression-type analyses.* Methods in Ecology and Evolution, 2016. **7**(6): p. 636-645.
77. Hsieh, Y.-Y.P., et al., *Widespread fungal-bacterial competition for magnesium enhances antibiotic resistance.* bioRxiv, 2023: p. 2023.10.25.563990.
78. Fukami, T., E.A. Mordecai, and A. Ostling, *A framework for priority effects.* Journal of Vegetation Science, 2016. **27**(4): p. 655-657.
79. Drake, J.A., *Community-Assembly Mechanics and the Structure of an Experimental Species Ensemble.* The American Naturalist, 1991. **137**(1): p. 1-26.
80. Cheong, J.Z.A., et al., *Priority effects dictate community structure and alter virulence of fungal-bacterial biofilms.* Isme j, 2021. **15**(7): p. 2012-2027.
81. Olsen, N.M.C., et al., *Priority of Early Colonizers but No Effect on Cohabitants in a Synergistic Biofilm Community.* Front Microbiol, 2019. **10**: p. 1949.
82. O'Brien, T.J., W. Figueroa, and M. Welch, *Decreased efficacy of antimicrobial agents in a polymicrobial environment.* The ISME Journal, 2022. **16**(7): p. 1694-1704.
83. Phuengmaung, P., et al., *Coexistence of Pseudomonas aeruginosa With Candida albicans Enhances Biofilm Thickness Through Alginate-Related Extracellular Matrix but Is Attenuated by N-acetyl-l-cysteine.* Front Cell Infect Microbiol, 2020. **10**: p. 594336.
84. Grainha, T., et al., *Unraveling Pseudomonas aeruginosa and Candida albicans Communication in Coinfection Scenarios: Insights Through Network Analysis.* Frontiers in Cellular and Infection Microbiology, 2020. **10**.
85. Quinn Rebecca, J., et al., *Periodically Disturbing the Spatial Structure of Biofilms Can Affect the Production of an Essential Virulence Factor in Pseudomonas aeruginosa.* mSystems, 2021. **6**(5): p. 10.1128/msystems.00961-21.
86. Gao, B., et al., *Tracking Polymicrobial Metabolism in Cystic Fibrosis Airways: Pseudomonas aeruginosa Metabolism and Physiology Are Influenced by Rothia mucilaginosa-Derived Metabolites.* mSphere, 2018. **3**(2): p. 10.1128/msphere.00151-18.
87. Lim, Y.W., et al., *Mechanistic Model of Rothia mucilaginosa Adaptation toward Persistence in the CF Lung, Based on a Genome Reconstructed from Metagenomic Data.* PLOS ONE, 2013. **8**(5): p. e64285.

88. Baishya, J. and C.A. Wakeman, *Selective pressures during chronic infection drive microbial competition and cooperation.* npj Biofilms and Microbiomes, 2019. **5**(1): p. 16.
89. Sugimoto, S., et al., *Staphylococcus epidermidis Esp degrades specific proteins associated with Staphylococcus aureus biofilm formation and host-pathogen interaction.* J Bacteriol, 2013. **195**(8): p. 1645-55.
90. Niggli, S. and R. Kümmerli, *Strain Background, Species Frequency, and Environmental Conditions Are Important in Determining Pseudomonas aeruginosa and Staphylococcus aureus Population Dynamics and Species Coexistence.* Applied and Environmental Microbiology, 2020. **86**(18): p. e00962-20.
91. Díaz-Pérez, S.P., et al., *Pathogenesis in Pseudomonas aeruginosa PAO1 Biofilm-Associated Is Dependent on the Pyoverdine and Pyocyanin Siderophores by Quorum Sensing Modulation.* Microb Ecol, 2022.
92. Reszka, K.J., et al., *Oxidation of pyocyanin, a cytotoxic product from Pseudomonas aeruginosa, by microperoxidase 11 and hydrogen peroxide.* Free Radic Biol Med, 2004. **36**(11): p. 1448-59.
93. Hazlett, H.F., et al., *Altered iron metabolism in cystic fibrosis macrophages: the impact of CFTR modulators and implications for Pseudomonas aeruginosa survival.* Scientific Reports, 2020. **10**(1): p. 10935.
94. Filipow, N., et al., *The impact of genetic background during laboratory evolution of Pseudomonas aeruginosa in a cystic fibrosis-like environment.* Evolution, 2024. **78**(3): p. 566-578.
95. Lenski, R.E., *Experimental evolution and the dynamics of adaptation and genome evolution in microbial populations.* The ISME Journal, 2017. **11**(10): p. 2181-2194.
96. Blount, Z.D., C.Z. Borland, and R.E. Lenski, *Historical contingency and the evolution of a key innovation in an experimental population of Escherichia coli*. Proceedings of the National Academy of Sciences, 2008. **105**(23): p. 7899-7906.
97. Alam, F., et al., *Candida albicans enhances meropenem tolerance of Pseudomonas aeruginosa in a dual-species biofilm.* Journal of Antimicrobial Chemotherapy, 2019. **75**(4): p. 925-935.
98. Kahl, L.J., et al., *Interkingdom interactions between Pseudomonas aeruginosa and Candida albicans affect clinical outcomes and antimicrobial responses.* Current Opinion in Microbiology, 2023. **75**: p. 102368.
99. Rahdar, H.A., et al., *Correlation between biofilm formation and carbapenem resistance among clinical isolates of Klebsiella pneumoniae.* Ethiop J Health Sci, 2019. **29**(6): p. 745-750.
100. Bottery, M.J., J.W. Pitchford, and V.-P. Friman, *Ecology and evolution of antimicrobial resistance in bacterial communities.* The ISME Journal, 2020. **15**(4): p. 939-948.

101. Vestweber, P.K., et al., *The interplay of Pseudomonas aeruginosa and Staphylococcus aureus in dual-species biofilms impacts development, antibiotic resistance and virulence of biofilms in in vitro wound infection models.* PLoS One, 2024. **19**(5): p. e0304491.
102. Dhekane, R., S. Mhade, and K.S. Kaushik, *Adding a new dimension: Multi-level structure and organization of mixed-species Pseudomonas aeruginosa and Staphylococcus aureus biofilms in a 4-D wound microenvironment.* Biofilm, 2022. **4**: p. 100087.
103. Zhang, K., et al., *Effect of Candida albicans' supernatant on biofilm formation and virulence factors of Pseudomonas aeruginosa through las/rhl System.* BMC Microbiology, 2025. **25**(1): p. 60.
104. Natalini, J.G., S. Singh, and L.N. Segal, *The dynamic lung microbiome in health and disease.* Nature Reviews Microbiology, 2023. **21**(4): p. 222-235.